Acknowledgements

This work was partly supported by the National Food Research Institute of Japan (project: Development of evaluation and management methods for supply of safe, reliable and functional food and farm produce) and Japanese Ministry of Health, Labour and Welfare (H19-011).

The authors thank for Tatsuya Ishikawa for MLVA data analyses.

References

Adair, D.M., Worsham, P.L., Hill, K.K., Klevytska, A.M., Jackson, P.J., Friedlander, A.M., Keim, P., 2000. Diversity in a variable-number tandem repeat from *Yersinia pestis*. J. Clin. Microbiol. 38, 1516–1519.

Arakawa, E., Murase, T., Shimada, T., Okitsu, T., Yamai, S., Watanabe, H., 1999. Emergence and prevalence of a novel *Vibrio parahaemolyticus* O3:K6 clone in Japan. Jpn. J. Infect. Dis. 52, 246–247.

Bag, P.K., Nandi, S., Bhadra, R.K., Ramamurthy, T., Bhattacharya, S.K., Nishibuchi, M., Hamabata, T., Yamasaki, S., Takeda, Y., Nair, G.B., 1999. Clonal diversity among recently emerged strains of *Vibrio parahaemolyticus* O3:K6 associated with pandemic spread. J. Clin. Microbiol. 37, 2354–2357.

Benson, G., 1999. Tandem repeats finder: a program to analysis DNA sequences. Nucleic Acids Res. 27, 573–580.

Centers for Disease Control and Prevention, 1999. Outbreak of *Vibrio parahaemolyticus* infection associated with eating raw oysters and clams harvested from Long Island Sound — Connecticut, New Jersey, and New York, 1998. Morbid. Mortal. Weekly Rep. 48, 48–51.

Chowdhury, N.R., Stine, O.C., Morris, J.G., Nair, G.B., 2004. Assessment of evolution of pandemic *Vibrio parahaemolyticus* by multilocus sequence typing. J. Clin. Microbiol. 42, 1280–1282.

Chowdhury, N.R., Chakraborty, S., Ramamurthy, T., Nishibuchi, M., Yamasaki, S., Takeda, Y., Nair, G.B., 2000. Molecular evidence of clonal *Vibrio parahaemolyticus* pandemic strains. Emerg. Infect. Dis. 6, 631–636.

DePaola, A., Ulaszek, J., Kaysner, C.A., Tenge, B.J., Nordstrom, J.L., Wells, J., Puhr, N., Gendel, S.M., 2003. Molecular, serological, and virulence characteristics of *Vibrio parahaemolyticus* isolated from environmental, food, and clinical sources in North America and Asia. Appl. Environ. Microbiol. 69, 3999–4005.

Gendel, S.M., Ulaszek, J., Nishibuchi, M., DePaola, A., 2001. Automated ribotyping differentiates *Vibrio parahaemolyticus* O3:K6 strains associated with a Texas outbreak from other clinical strains. J. Food Prot. 64, 1617–1620.

Hara-Kudo, Y., Sugiyama, K., Nishibuchi, M., Chowdhury, A., Yatsuyanagi, J., Ohtomo, Y., Saito, A., Nagano, H., Nishina, T., Nakagawa, H., Konuma, H., Miyahara, M., Kumagai, S., 2003. Prevalence of pandemic thermostable direct hemolysin-producing *Vibrio parahaemolyticus* O3:K6 in seafood and the coastal environment in Japan. Appl. Environ. Microbiol. 69, 3883–3891.

Honda, T., Iida, T., 1993. The pathogenicity of *Vibrio parahaemolyticus* and the role of the thermostable direct hemolysin and related hemolysins. Rev. Med. Microbiol. 4, 106–113.

Keim, P., Price, L.B., Klevytska, A.M., Smith, K.L., Schupp, J.M., Okinaka, R., Jackson, P.J., Hugh-Jones, M.E., 2000. Multiple-locus variable-number tandem repeat analysis reveals genetic relationships within *Bacillus anthracis*. J. Bacteriol. 182, 2928–2936.

Lindstedt, B.A., Vardund, T., Kapperud, G., 2004a. Multiple-locus variable-number tandem-repeat analysis of *Escherichia coli* O157 using PCR multiplexing and multi-colored capillary electrophoresis. J. Microbiol. Methods 58, 213–222.

Lindstedt, B.A., Vardund, T., Aas, L., Kapperud, G., 2004b. Multiple-locus variable-number tandem-repeats analysis of *Salmonella enterica* subsp. *enterica* serovar Typhimurium using PCR multiplexing and multicolor capillary electrophoresis. J. Microbiol. Methods 59, 163–172.

Makino, K., Oshima, K., Kurokawa, K., Yokoyama, K., Uda, T., Tagomori, K., Iijima, Y., Najima, M., Nakano, M., Yamashita, A., Kubota, Y., Kimura, S., Yasunaga, T., Honda, T., Shinagawa, H., Hattori, M., Iida, T., 2003. Genomic sequence of *Vibrio parahaemolyticus*: a pathogenic mechanism distinct from that of *V. cholerae*. Lancet 361, 743–749.

Marshall, S., Clark, C.G., Wang, G., Mulvey, M., Kelly, M.T., Johnson, W.M., 1999. Comparison of molecular methods for typing *Vibrio parahaemolyticus*. J. Clin. Microbiol. 37, 2473–2478.

Matsumoto, C., Okuda, J., Ishibashi, M., Iwanaga, M., Garg, P., Rammamurthy, T., Wong, H., DePaola, A., Kim, Y.B., Albert, M.J., Nishibuchi, M., 2000. Pandemic spread of an O3:K6 clone of *Vibrio parahaemolyticus* and emergence of related strains evidenced by arbitrarily primed PCR and *toxRS* sequence analyses. J. Clin. Microbiol. 38, 578–585.

Metzgar, D., Thomas, E., Davis, C., Field, D., Wills, C., 2001. The microsatellites of *Escherichia coli*: rapidly evolving repetitive DNAs in a non-pathogenic prokaryote. Mol. Microbiol. 39, 183–190.

Murray, M., G., Thompson, W.F., 1980. Rapid isolation of high molecular weight plant DNA. Nucl. Acids Res. 8, 4321–4325.

Naim, R., Yanagihara, I., Iida, T., Honda, T., 2001. *Vibrio parahaemolyticus* thermostable direct hemolysin can induce an apoptotic cell death in Rat-1 cells from inside and outside of the cells. FEMS Microbiol. Lett. 195, 237–244.

Nasu, H., Iida, T., Sugahara, T., Yamaichi, Y., Park, K., Yokoyama, K., Makino, K., Shinagawa, H., Honda, T., 2000. A filamentous phage associated with recent pandemic *Vibrio parahaemolyticus* O3:K6 strains. J. Clin. Microbiol. 38, 2156–2161.

Noller, A.C., McEllistrem, M.C., Pacheco, A.G.F., Boxrud, D.J., Harrison, L.H., 2003. Multilocus variable-number tandem repeat analysis distinguishes outbreak and sporadic *Escherichia coli* O157:H7 isolates. J. Clin. Microbiol. 41, 5389–5397.

Okuda, J., Ishibashi, M., Hayakawa, E., Nishino, T., Takeda, Y., Mukhopadhyay, A.K., Garg, S., Bhattacharya, S.K., Nair, G.B., Nishibuchi, M., 1997. Emergence of a unique O3:K6 clone of *Vibrio parahaemolyticus* in Calcutta, India, and isolation of strains from the same clonal group from Southeast Asian travelers arriving in Japan. J. Clin. Microbiol. 35, 3150–3155.

Okura, M., Osawa, R., Iguchi, A., Arakawa, E., Terajima, J., Watanabe, H., 2003. Genotypic analyses of *Vibrio parahaemolyticus* and development of a pandemic group-specific multiplex PCR assay. J. Clin. Microbiol. 41, 4676–4682.

Onteniente, L., Brisse, S., Tassios, P.T., Vergnaud, G., 2003. Evaluation of polymorphisms associated with tandem repeats for *Pseudomonas aeruginosa* strain typing. J. Clin. Microbiol. 41, 4991–4997.

Sabat, A., Krzyszton-Russjan, J., Strzalka, W., Filipek, R., Kosowska, K., Hryniewicz, W., Travis, J., Potempal, J., 2003. New method for typing *Staphylococcus aureus* strains: multiple-locus variable-number tandem repeat analysis of polymorphism and genetic relationships of clinical isolates. J. Clin. Microbiol. 41, 1801–1804.

Sambrook, J.E., Fritsch, F., Maniatis, T.S., 1989. Molecular cloning: A Laboratory Manual, 2nd edn. Cold Spring Harbor Laboratory, Cold Spring Harbor, New York.

Shinoda, S., Matsuoka, H., Tsuchie, T., Miyoshi, S., Yamamoto, S., Taniguchi, H., Mizuguchi, Y., 1991. Purification and characterization of a lecithin-dependent hemolysin from *Escherichia coli* transformed by a *Vibrio parahaemolyticus* gene. J. Gen. Microbiol. 137, 2705–2711.

Sreenu, V.A., Alevoor, V., Nagaraju, J., Nagarajaram, H.A., 2003. MICdb: database of prokaryotic microsatellites. Nucleic Acids Res. 31, 106–108.

Taniguchi, H., Kubomura, S., Hirano, H., Mizue, K., Ogawa, M., Mizuguchi, Y., 1990. Cloning and characterization of a gene encoding a new thermostable hemolysin from *Vibrio parahaemolyticus*. FEMS Microbiol. Lett. 67, 339–345.

Truman, R., Fontes, A.B., de Miranda, A.B., Suffys, P., Gillis, T., 2004. Genotypic variation and stability of for variable-number tandem repeats and their suitability for discriminating strains of *Mycobacterium leprae*. J. Clin. Microbiol. 42, 2558–2565.

Wong, H.C., Liu, S.H., Wang, T.K., Lee, C.L., Chiou, C.S., Liu, D.P., Nishibuchi, M., Lee, B.K., 2000. Characteristics of Vibrio parahaemolyticus O3:K6 from Asia. Appl. Environ. Microbiol. 66, 3981–3986.

Yeung, P.S.M., Hayes, M.C., DePaola, A., Kaysner, C.A., Kornstein, L., Boor, K.J., 2002. Comparative phenotypic, molecular, and virulence characterization of *Vibrio parahaemolyticus* O3:K6 isolates. Appl. Environ. Microbiol. 68, 2901–2909.

J Ind Microbiol Biotechnol (2007) 34:685–688
DOI 10.1007/s10295-007-0231-7

SHORT COMMUNICATION

Visualization of yeast single-cells on fabric surface with a fluorescent glucose and their isolation for culture

Kohtaro Fujioka · Philip Geis · Mikako Saito · Hideaki Matsuoka

Received: 25 March 2007 / Accepted: 20 May 2007 / Published online: 14 June 2007

Abstract An ultra-deep focusing range (UDF) fluorescent microscope system has been combined with a micromanipulation system to develop a viable cell detection-identification system applicable to microbes on environmental surfaces and products. *Candida albicans* yeast cells on a fabric sample surface were viably stained with a fluorescent glucose derivative, 2-[*N*-(7-nitrobenz-2-oxa-1,3-diazol-4-yl)amino]-2-deoxy glucose (2-NBDG) and detected with a UDF fluorescent microscope. Visualized single-cells of *C. albicans* were picked in a glass microcapillary and transferred onto an agar medium. After the culture, the colony was assayed for DNA sequence to identify the isolate. This demonstrates a potential application to the study of unknown environmental microorganisms.

Keywords Ultra-deep focusing range (UDF) fluorescent microscope · Single-cell manipulation · Fluorescent glucose derivative · Viable cell imaging

K. Fujioka
Kobe Technical Center, Procter & Gamble Far East, Inc., 17, Koyo-cho Naka 1-Chome, Higashinada-ku, Kobe 658-0032, Japan

K. Fujioka · M. Saito · H. Matsuoka (✉)
Department of Biotechnology and Life Science, Tokyo University of Agriculture and Technology, Koganei, Tokyo 184-8588, Japan
e-mail: bio-func@cc.tuat.ac.jp

P. Geis
Sharon Woods Technical Center, The Procter & Gamble Co., 11530 Reed Hartman Highway, Cincinnati, OH 45242, USA

Introduction

Quantitative and qualitative analyses of environmental microorganisms have been attempted with various methods and approaches [2, 3, 7, 13, 15]. Where effective, these usually require days to obtain the results and fail to connect the visual to microbial species. Currently, urgent needs exist in the detection of food pathogens in cooking environment [11, 17] and microbial growth in damp garments after the laundry washing process [10, 14]. To meet these needs, we have recently developed a ultra-deep focusing range (UDF) fluorescent microscope system and applied it successfully to the evaluation of microbial cell removal from fabrics [4], and to the automatic mapping of viable microbial cells being distributed in the surface layer of cotton fabrics [5]. The next step is to isolate those single-cells for their identification. Once the single-cells have been isolated, they can be cultured on an agar medium. Thus formed colonies may be used for further investigation including DNA analysis and metabolism analysis. This research demonstrates the detection of single-cells of *Candida albicans* on fabrics and their isolation for the culture.

Materials and methods

Microbial strains

Candida albicans, which is one of the key human pathogens [6, 16] and contaminants in cosmetic industry [1] was chosen as a microbial strain for this study. Seed cultures of *C. albicans* ATCC 10231 were prepared from frozen stocks from MICROBANK kit (Pro-lab Diagnostics, Toronto, Canada) and cultured in the 1/10th strength Trypticase Soy Broth (1/10 TSB) to approximately 10^6 cfu/ml. Fabric

samples used are Kanakin 3 [8]. Fabric swatches were prepared as 1.0 cm × 1.0 cm squares, wrapped with aluminum foil, autoclaved at 121°C for 15 min, and dried under sterile conditions.

Fluorescent glucose derivative treatments

Synthesis of 2-[*N*-(7-nitrobenz-2-oxa-1,3-diazol-4-yl)amino]-2-deoxy glucose (2-NBDG) was conducted following the protocol described elsewhere [18].

A 200 µl inoculum of the seed culture containing about 5×10^6 cells of *C. albicans* was inoculated onto a swatch, and the swatch was placed on Trypticase Soy Agar (TSA) plates. After incubation at 33°C for 1 h, the remaining aqueous liquid on the swatch was removed by Ultrafree-MC centrifuging treatment (6,000 rpm × 30 s). To obtain individual components amendable to microscopic observations, the centrifuged swatch was untied and dissected to individual strings with pre-sterilized tweezers. The individual fabric strings were set on a glass slide upon which a square grid has been imprinted. Approximately 2.0 ml of 0.2% agarose solution containing 12 µM 2-NBDG was prepared in molten condition at 46°C, and poured onto the reassembled fabric strings on the slide glass. The glass slide was kept in a petri-dish and incubated for 1 h at 33°C to facilitate the uptake of 2-NBDG by *C. albicans*.

Microscope and manipulation systems

After incubation, the glass slide was examined with a UDF fluorescent microscope system. The detailed components of the UDF fluorescent system are described previously [4, 5]. Ultra long distance industrial optical lenses (CFI Plan EPI SLWD 50 and 30, NIKON Co., working distance 17.0 and 24.0 mm, respectively) and a semi-automatic cell injection manipulator (InjectMan NI2, Eppendorf Co.) were integrated to assemble a cell manipulation system (Fig. 1). InjectMan NI2 was fixed on the UDF system stage with steel frames.

To prepare glass capillaries for the yeast cell manipulation, borosilicate glass tubes (BF100-78-10, diameter 1.0–0.78 mm, Sutter Instrument Co.) were pulled with a laser puller (P-2000, Sutter Instrument Co.), sterilized with anhydrous ethyl alcohol and dried in a dry oven at 50°C for 48 h. For cell manipulation, a sterile silicone tube 2 mm in diameter was connected to the capillary and to the InjectMan NI2.

DNA sequence analyses

Isolated cells were incubated on TSA plates at 33°C for 48 h to prepare sufficient cell mass for DNA sequence analyses. The harvested cells were transferred to a 1.8 mL serum tube and frozen in liquid nitrogen. Frozen cells were treated with homogenization pestle to break the cell wall. This process was repeated two times. DNA was extracted from the homogenate with E.N.Z.A. Fungal DNA Kit (Omega Bio-tek, Inc.). PCR amplification was conducted on the 26S rDNA D1/D2 regions [9] with primers NL-1(5′-CGATATCAATAAGCGGAGGAAAAG) and NL-4(5′-GGTCCGTGTTTCAAGACGG) [12] with a thermal cycler (PTC-200 Peltier Thermal Cycler, MJ Research Co.) under the conditions of 95°C × 10 s + 50°C × 60 s + 70°C × 60 s (denaturation, annealing, and extension, 30 cycles), and 72°C × 10 min (extension) . The PCR products obtained were purified with QIA quick PCR Purification Kit (QIAGEN Co.) and DNA sequence analyses were done with PRISM3100 genetic Analyzer (ABI Co.).

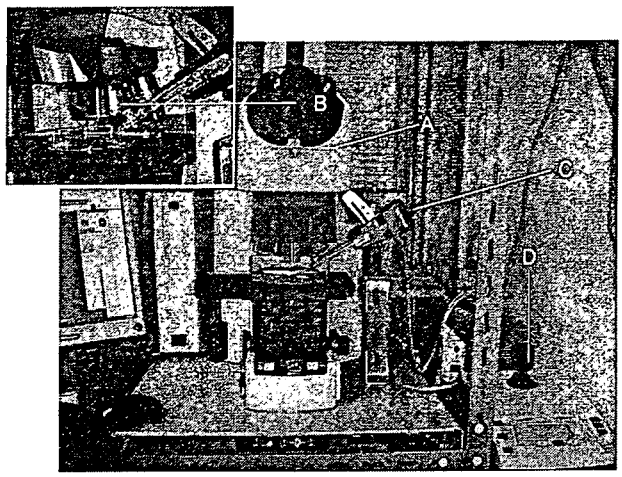

Fig. 1 A UDF fluorescent microscope system with a cell manipulation system. *A* microscope, *B* ultra long distance industrial optical lens, *C* manipulator, *D* operation module of manipulator

Results and discussion

The fluorescent images indicate viabile cells attaching on the surface of fabrics and their morphologies can be recognized (Fig. 2). Following this cell detection, a glass capillary was inserted in molten agar and placed adjacent to cells (Fig. 3a, fluorescent image). Then the cells were sucked into the capillary (Fig. 3b, c). The isolated cells were cultured as described and subjected to DNA sequence analysis at D1/D2 domain in 26S rDNA to certify that the originally inoculated strain was recovered. The gel electrophoresis band picture of the PCR product is shown in Fig. 4. A single band appeared at the same position as that obtained from the originally inoculated cells. The DNA sequence analyses data of 572 bp indicated 100% sequence matching. These indicate the clear traceability of the inoculated strain.

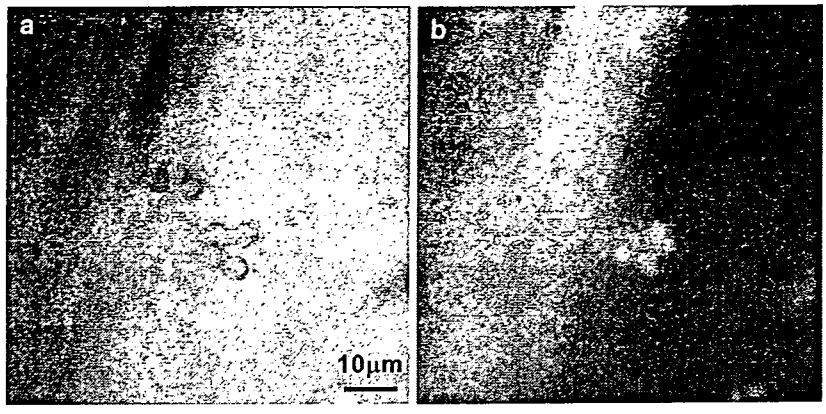

Fig. 2 Microscopic images of *Candida albicans* observed on fabric before cell isolation. **a** Optical image, **b** fluorescent image

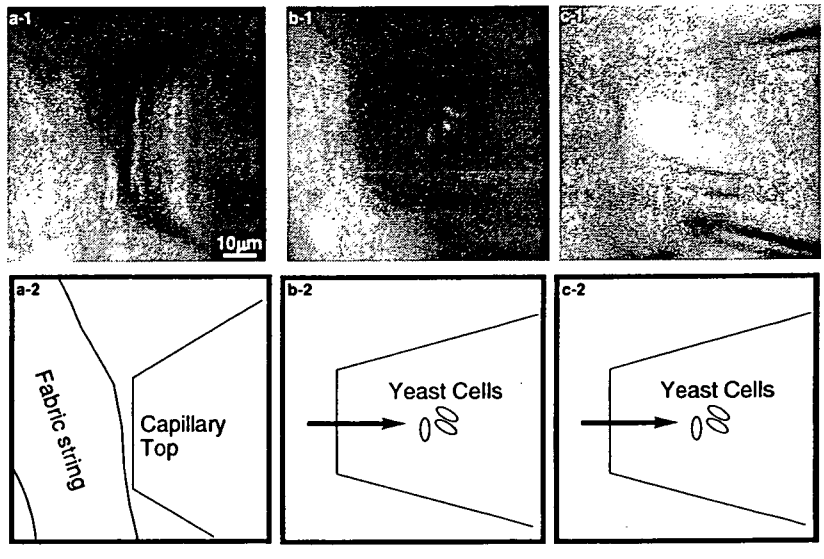

Fig. 3 Cell isolation procedure. **a** Glass capillary inserted to molten agar coating the fabric (optical image). **b, c** *C. albicans* cells sucked in a capillary stored in the glass capillary [optical image (**b**) and fluorescent image (**c**)]

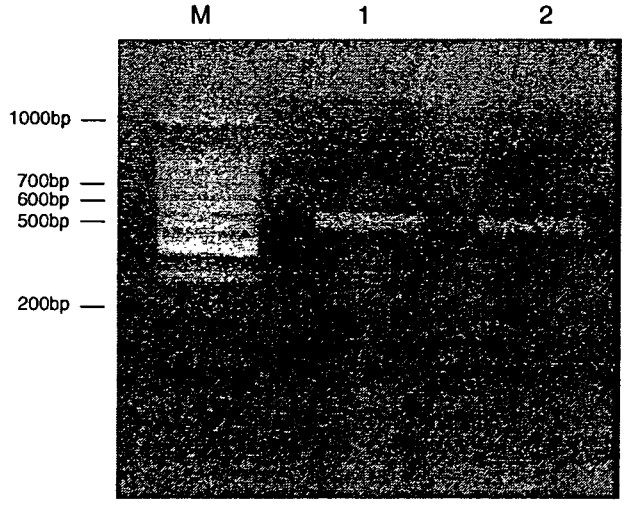

Fig. 4 Gel electrophoresis band picture of the PCR products. A total of 2% agarose, TAE Buffer, *M* Takara 100 bp ladder as a marker, *1* DNA derived from the inoculated strain, *2* DNA derived from the manipulated/isolated strain

Successful visualization and manipulation demonstrate the applicability of the present system to the detection of very low numbers of microbial cells and for their successive culture. The first is to detect viable cells rapidly and the next is to investigate them carefully depending upon the necessity.

Single-cell manipulation supporting technologies have recently gained marked progress [19, 20] and therefore the present system may be advanced to a higher throughput system in response to practical needs.

Acknowledgments This research was supported by the Microbial Visualization Community of Practice in The Procter & Gamble Company. H.M. acknowledges supports from Grant-in-aid for Scientific Research for the Promotion of Safety and Security of Foods, The Ministry of Health, Labor, and Welfare, and from CREST of Japan Science and Technology Agency.

References

1. Abedelaziz A-A, Ashour M-S (1987) Microbial contamination of hexetidine mouth wash. Zentrabl Bakteriol Mikrobiol Hyg [B] 184:262–268
2. Brown D-F, Dupont J, Dumont F, menanteau C, Pommepuy M (2004) Calibration of the impedance method for rapid quantitative estimation of *Escherichia coli* in live marine bivalve molluscs. J Appl Microbiol 4:894–902

3. Esioubu N (2006) Use of peptide nucleic acid probes for rapid detection and enumeration of viable bacteria in recreational waters and beach sand. Methods Mol Biol 345:131–140
4. Fujioka K, Kozone I, Saito M, Matsuoka H (2006) Rapid evaluation of the efficacy of microbial cell removal from fabrics. J Ind Microbiol Biotechnol 33:995–1002
5. Fujioka K, Kozone I, Saito M, Matsuoka H (2007) Automatic mapping of viable microbial cells being distributed in the surface layer of cotton fabrics. Biocontrol Sci 12(1):31–34
6. Hansson C, Jekler J, Swanbeck G (1985) *Candida albicans* infections in leg ulcers and surrounding skin after the use of ointment impregnated stockings. Acta Derm Venereol 65:424–427
7. Jimenez L (2001) Molecular diagnosis of microbial contamination in cosmetic and pharmaceutical products: a review. J AOAC Int 84:671–675
8. JIS L0803 (1998) Standard adjacent fabrics for straining of colour fastness test
9. Kurtzman C-P, Robnett C-J, (1998) Identification and phylogeny of ascomycetous yeasts from analysis of nuclear large subunit (26S) ribosomal DNA partial sequences. Antonie van Leeuwenhoek 73:331–371
10. Marples R-R, Towers A-G (1979) A laboratory model for the investigation of contact transfer of micro-organisms. J Hyg (Lond) 82:237–248
11. Nielsen P, Brumbaugh E, Kananen L (2002) Evaluation of the use of liquid dishwashing compounds to control bacteria in kitchen sponges. J AOAC Int 85:107–112
12. O'Donnell K, (1993) *Fusarium* and its near relatives. In: Reynolds DR, Taylor JW (ed) The fungal holomorph: mitotic, meiotic and pleomorphic speciation in fungal systematics. CAB International, Wallingford, pp 225–233
13. Odumeru J-A, Belvedere J (2002) Evaluation of the MicroFoss system for enumeration of total viable count, *Escherichia coli* and coliforms in ground beef. J Microbiol Methods 50:33–38
14. Patrick D-R, Findon G, Miller T-E (1997) Residual moisture determines the level of touch-contact-associated bacterial transfer following hand washing. Epidemiol Infect 119:319–325
15. Ren Z, Hsiehi Y-H (2005) Real-time determination of microbial activity of pasteurized fluid milk using a novel microrespirometer method. J AOAC Int 88:1756–1761
16. Scherer S, Magee P-T (1990) Genetics of *Candida albicans*. Microbiol Rev 54:226–241
17. Venkitanarayanan K-S, Ezeike G-O, Hung Y-C, Doyle M-P (1999) Inactivation of *Escherichia coli* O157:H7 and *Listeria monocytogenes* on plastic kitchen cutting boards by electrolyzed oxidizing water. J Food Prot 62:857–860
18. Yoshioka K, Takahashi H, Homma T, Saito M, Oh K-B, Nemoto Y, Matsuoka H (1996) A novel fluorescent derivative of glucose applicable to the assessment of glucose uptake activity of *Escherichia coli*. Biochim Biophys Acta 1289:5–9
19. Matsuoka H, Komazaki T, Mukai Y, Shibusawa M, Akane H, Chaki A, Uetake N, Saito M (2005) High throughput easy microinjection with a single-cell manipulation supporting robot. J Biotechnol 116:185–194
20. Matsuoka H, Yamada Y, Matsuoka K, Saito M (2006) High throughput microinjection technology for the single-cell analysis of BY-2 in vivo. In: Nagata T, Matsuoka K, Inzé D (eds) Tobacco BY-2 cells: from cellular dynamics to omics. Springer, Berlin, pp 339–346

Biocontrol Science, 2007, Vol. 12, No. 1, 31−34

Note

Automatic Mapping of Viable Microbial Cells Distributed in the Surface Layer of Cotton Fabrics

KOHTARO FUJIOKA[1, 2], IKUKO KOZONE[2], MIKAKO SAITO[2], AND HIDEAKI MATSUOKA[2]*

[1]*Kobe Technical Center, Procter & Gamble Far East, Inc., 17, Koyo-cho Naka 1-Chome, Higashinada-ku, Kobe 658-0032, Japan*
[2]*Department of Biotechnology and Life Science, Tokyo University of Agriculture and Technology, Koganei, Tokyo 184-8588, Japan*

Received 17 October 2006/Accepted 18 January 2007

Viable microbial cells distributed in a 130 μm thick surface layer of cotton fabrics were stained with a fluorescent glucose, 2-[*N*-(7-nitrobenz-2-oxa-1,3-diazol-4-yl)amino]-2-deoxy-D-glucose (2-NBDG), and automatically mapped with an ultra-deep focusing range microscope (UDF) system. The software of the UDF system was upgraded and the number of *Candida albicans* cells could be counted at a higher precision than before. Bacterial cells of *Pseudomonas fluorescens*, *Serratia marcescens*, and *Citrobacter freundii*, which were smaller than 1-2 μm, were successfully mapped for the first time. These results indicate the practical importance of the present method in the evaluation of the antibacterial properties of fabrics and the efficacy of washing.

Key words : Ultra-deep focusing range (UDF) fluorescent microscope/A fluorescent glucose/ Viable cell imaging/Cell deposition on fabrics.

Visualization *in situ* of viable microbial cells on the surface of fabrics is of practical importance and has been important for the evaluation of antibaterial properties of fabrics (JIS L1902, 2002; Borkow and Gabbay, 2004; Cen et al., 2004) and the efficacy of washing (Petrocci and Clarke, 1969; JIS L0844, 1997; ASTM E2274-03, 2004). One of the key challenges in conducting such an evaluation is to deal with the topology of fabric surfaces which is not flat at the micrometer scale but composed of many fibers to form a complex structure. Microbial cells are deposited on thin fibers or entrapped deeply between fibers. To detect these cells within a deep focusing range simultaneously, confocal microscopy (Roldán et al., 2004; Staudt et al., 2004), decomvolution microscopy (McNally et al., 1999), and other methods (Burton, 2003; Buda et al., 2005) have been proposed and in fact some models based on these principles are commercially available. However it was difficult to modify available models at a reasonable cost to fit our specific resolutional purpose. Thus we developed a novel microscopic system with an UDF system (Fujioka et al., 2006). In combination with the staining of viable cells with a fluorescent glucose derivative, 2-NBDG (Yoshioka et al., 1996; Matsuoka et al., 2003), the UDF system was found to be useful for the rapid evaluation of the efficacy of microbial cell removal (EMR) from fabrics in the specific case of *Candida albicans* microbes greater than 5 μm.

From a practical viewpoint, however, it is essential to establish a spatial resolution as high as 1-2 μm. In this study, we have critically revised the principal image processing software. As described below, the mapping of *C. albicans* has been successfully performed with much higher resolution. The mappings of bacterial cells smaller than 1-2 μm are also demonstrated.

Seed cultures of *C. albicans* ATCC10231, the environmental isolates of *Pseudomonas fluorescens*,

*Corresponding author. Tel : +81-42-388-7029, Fax : +81-42-387-1503, e-mail: mhide@cc.tuat.ac.jp

Serratia marcescens, and *Citrobacter freundii* were prepared from respective frozen stocks with MICROBANK kit (Pro-lab Diagnostics, Toronto, Canada) and cultured in 1/10 strength Trypticase Soy Broth (1/10 TSB) to approximately 10^6 cfu/ml. Fabric samples used were Kanakin 3 (JIS L0803, 1998), Cotton knit without a brightener, and Cotton 100 denim. These are differently knitted to form unique textures and certified by the Japan Spinners' Association. The fabric swatches were prepared as 1.0 cm × 1.0 cm squares, wrapped with aluminum foil, autoclaved at 121℃ for 15 min, and dried up under sterilized conditions. The synthesis of 2-NBDG was performed following the protocol described elsewhere (Yoshioka et al., 1996).

A 50 μl inoculum of the seed culture containing about 5×10^6 cells of *C. albicans* was inoculated onto each swatch, and the swatch was placed on Trypticase Soy Agar (TSA) plates. After the incubation at 33℃ for 16 h, each swatch was soaked in 9ml saline and vortexed for 5 min to remove most of the microbial cells from the each swatch. Thus we prepared swatch samples on which only small numbers of microbial cells remained. Each swatch was cut into 2 pieces (0.5 cm × 1.0 cm each). One piece (I) was used for the visualization experiment after being stained with 2-NBDG. The other piece (II) was used for the colony count assay only in the case of bacterial cells.

The conditions of 2-NBDG staining were as follows. A 400 μl aliquot of 12 μM 2-NBDG was placed on the fabric swatch piece (I). After incubation at 33℃ for 10 min, the remaining aqueous liquid was removed by Ultrafree-MC centrifuging treatment (6000 rpm × 30s). After that, a 100 μl of 30% formaldehyde (HCHO) solution was added with a pipette on the swatch and incubated at 33℃ for 1 min in order to fix the microbial cells. Immediately after that, the swatch was soaked in 9 ml saline for 5 min and centrifuged (6000 rpm × 30 s) to remove extracellular 2-NBDG. This washing with saline was repeated 2 times and microscopic observation with the UDF system was performed.

Previously we often encountered the image of a *C. albicans* cell indicated by an arrow in Fig. 1. In such a case, the single-cell emitted intense fluorescence at both ends and consequently was recognized as 2 cells in the automatic mapping. Such an image was due to a large vacuole that could hardly be stained by 2-NBDG. The increase in the spatial resolution, however, has enabled the recognition of such a case as a single-cell. Typical cases are observed at 4 positions in Fig. 2-Aa. These spots could be successfully registered as single-cells, respectively, as No. 1, 2, 5, and 8 in Fig. 2-Ab. A similar case is also observed in Fig. 2-Ba and registered as No. 5.

As may be observed in the Figs. 2-Ab, 2-Bb, and 2-

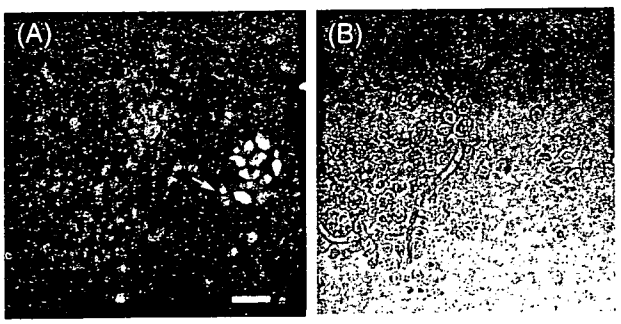

FIG. 1. Typical fluorescent pattern observed in *C. albicans* stained with 2-NBDG. (A) Fluorescent image, (B) Bright field image. Scale bar: 10 μm. The arrow indicates a typical image pattern of both ends emitting intense fluorescence. Observed with VC100 × oil objective lens through BV-2A filter.

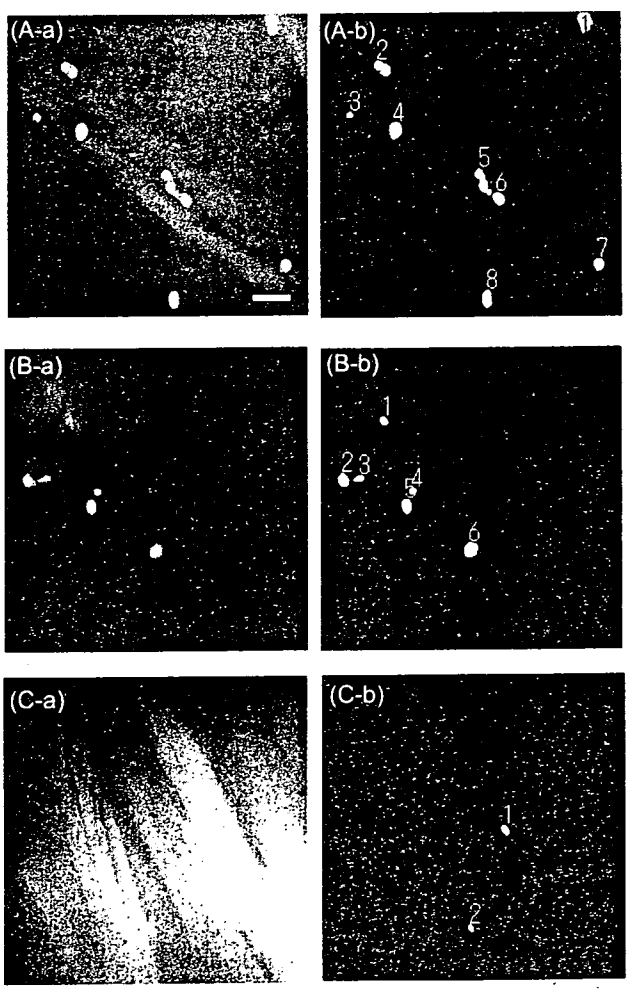

FIG. 2. Mapping of *C. albicans* in the surface layer of different cotton materials. (A) Kanakin3, (B) Cotton Knit without brightener, (C) Cotton 100 Denim. Scale bar: 10 μm.

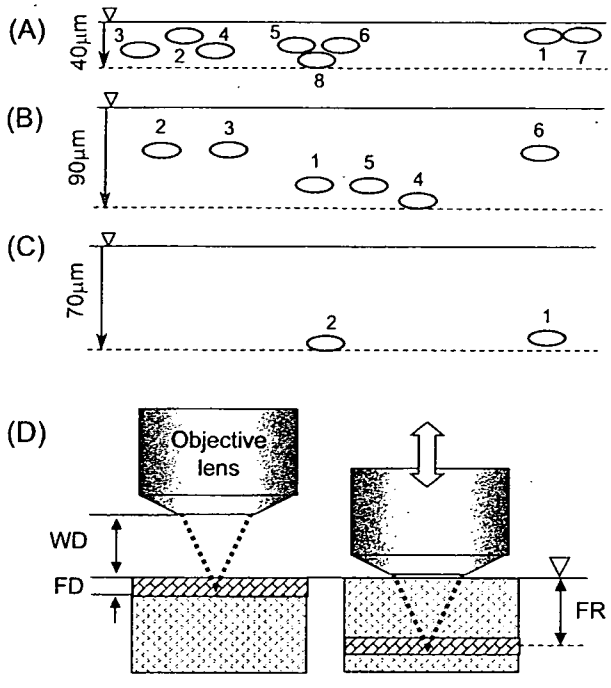

FIG. 3. Estimated depth of each cell from the fabric surface. Numbered cells in (A), (B), and (C) correspond to the numbered cells in (A), (B), and (C) of Fig.2, respectively. (D) Focusing range that can be observed simultaneously by the UDF system. ▽: Fabric surface, - - - in (A)~(C): Deepest cell level observed in respective cases, WD: Working distance (130 μm), FD: In-focus depth (a few μm), FR: Focusing Range (max 130 μm).

Cb, it is noticed that every fluorescent spot looks equally clear in outline and similar in size, though every cell does not necessarily exist in the same depth. The UDF system can integrate microscopic images from the surface to 130 μm depth at maximum (Fig. 3-D). Therefore the mapping data include the information of the depth of each cell. Based on these data, approximate positions of respective cells are shown in Figs. 3-A, 3-B, and 3-C. Such data are useful to estimate the degree of cell invasion into fabric matrices of different physical properties as well as their removal by washing.

Next is the automatic mapping of bacterial cells smaller than 2-3 μm. The objective lens was ×100 APO to zoom into the bacterial cell. In the case of Fig. 4-Aa, many fluorescent spots could be observed with similar fluorescent intensities. Thus every spot could be mapped as a light spot of similar size by adjusting the threshold level for the binarization at an appropriate level (Fig. 4-Ab). In the other two cases, only one cell was recognized as a light spot (Figs. 4-Ba, 4-Ca). According to the properly adjusted threshold level and the criteria for single-cell size, only this spot could be registered as a bacterial cell (Fig. 4-Bb, 4-

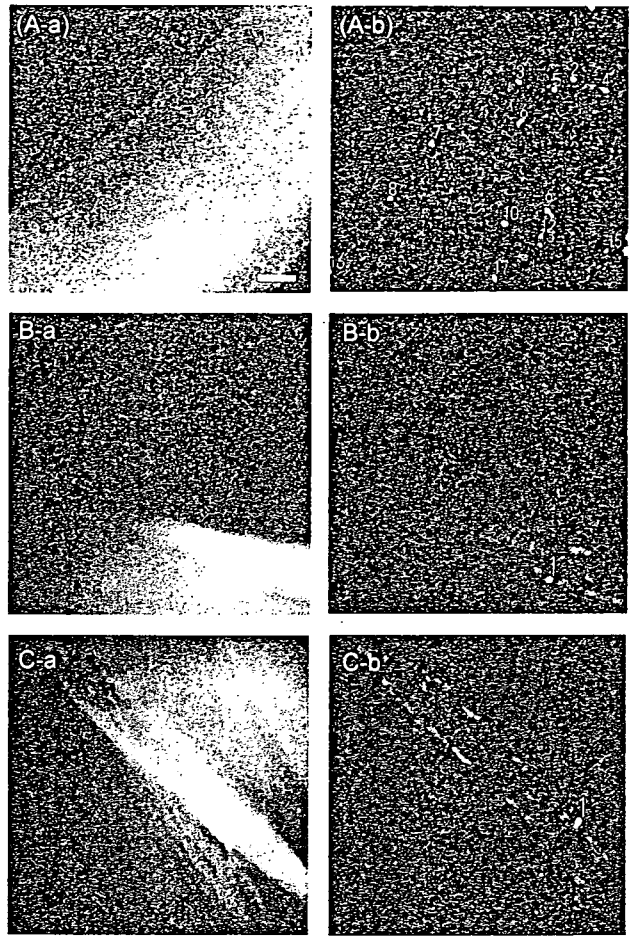

FIG. 4. Mapping of bacterial cells in the surface layer of Kanakin3. (A) *P. fluorescens*, (B) *S. marcescens*, (C) *C. freundii*. Observed with VC100×oil objective lens through BV-2A filter. Scale bar: 10 μm.

Cb).

Practically, it is necessary to confirm the quantitative relation between the cell numbers determined by the present method and by the conventional colony count method. However, the challenge of statistics regarding sample size still remained. In fact the area that was analyzed by the present method was too small to be compared to the colony count method. This problem will be resolved by the future development of an automatic scanning system for a fabric swatch of a much larger area.

Since only one cell is detected in Fig.4-B and 4-C respectively, it may be necessary to confirm by the colony count method that bacterial cells were actually remaining on/in the fabric swatch. The other halves (swatch piece (II)) used for Fig. 4 were assayed for viable cells according to the following protocol. The swatch piece (II) was immersed in 9 ml of 1/10 TSB and vortexed for 5 min and then taken out from the 1/10 TSB. A 0.5 ml aliquot of the 1/10 TSB

(suspension A) was mixed with TSA and poured in a dish for culturing at 33℃ for 72 h. Since the cell concentration in the suspension A was thought to be markedly small, suspension A was also incubated at 33℃ for another successive 48 h to increase it. A 1 00 μl aliquot of the resulting suspension (suspension B) was spread on a TSA plate and incubated at 33 ℃ for 24 h to count the colony number. As a result, after the incubation, no colony growth was observed on the TSA plates of suspension A. On the other hand, some growth was observed on the plates of suspension B (Fig.4-B: 44 cfu/plate, Fig.4-C: 55 cfu/plate). This supports the idea that the amounts of the residual levels of bacteria are very low.

In conslusion, the UDF system has been upgraded so that it may count automatically the cell number of *C. albicans* as well as smaller bacterial cells at a higher precision than before. The present results suggest the importance of the further development of a practical version of the UDF system.

Acknowledgments

This research was supported by the Microbial Visualization Community of Practice of the Procter & Gamble Company. The authors would like to thank Dr. P. Geis and Dr. S. Donaldson of the Procter & Gamble Company for holding constructive discussions with us and for reviewing the manuscript. We also thank Mr. Tottori of Kogaku Inc. for his support for and input into the microscopic system designs. One of the authors, H. Matsuoka, acknowledges support from Grant-in-aid for Scientific Research for the Promotion of Safety and Security of Foods, The Ministry of Health, Labor, and Welfare.

REFERENCES

ASTM E2274-03 (2004) Standard test method for evaluation of laundry sanitizers and disinfectants.

Borkow, G., and Gabbay, J. (2004) Putting copper into action: copper-impregnated products with potent biocidal activities. *FASEB J.*, **18**, 1728-1730.

Buda, A., Sands, C., and Jepson, M.-A. (2005) Use of fluorescence imaging to investigate the structure and function of intestinal M cells. *Adv. Drug Deliv. Rev.*, **57**, 123-134.

Burton, K. (2003) An aperture-shifting light-microscopic method for rapidly quantifying positions of cells in 3D matrices. *Cytometry*, **A54**, 125-131.

Cen, L., Neoh, K.-G., and Kang, E.-T. (2004) Antibacterial activity of cloth functionalized with N-alkylated poly(4-vinylpyridine). *J. Biomed. Mater. Res.*, **A71**, 70-80.

Fujioka, K., Kozone, I., Saito, M., and Matsuoka, H. (2006) Rapid evaluation of the efficacy of microbial cell removal from fabrics. *J. Ind. Microbiol. Biotechnol.*, **33**, 995-1002.

Japan Industrial Standard L0844 (1997) Test methods for colour fastness to washing and laundering.

Japan Industrial Standard L1902 (2002) Testing for antibacterial activity and efficacy on textile products.

Petrocci, A. M., and Clarke, P. (1969) Proposed test method for antimicrobial laundry additives. *J. of AOAC*, **52**, 836-842.

Roldán, M., Thomas, F., Castel, S., Quesada, A., and Hernández-Mariné, M. (2004) Noninvasive pigment identification in single cells from living phototrophic biofilms by confocal imaging spectrofluorometry. *Appl. Environ. Microbiol.*, **70**, 3745-3750.

Staudt, C., Horn, H., Hempel, D.-C., Neu, T.-R. (2004) Volumetric measurements of bacterial cells and extracellular polymeric substance glycoconjugates in biofilms. *Biotechnol. Bioeng.*, **88**, 585-592.

Matsuoka, H., Oishi, K., Watanabe, M., Kozone, I., Saito, M., and Igimi, S. (2003) Viable cell detection by the combined use of fluorescent glucose and fluorescent glycine. *Biosci. Biotechnol. Biochem.*, **67**, 2459-2462.

McNally, J.-G., Karpova, T., Cooper, J., and Conchello, J.-A. (1999) Three-dimensional imaging by deconvolution microscopy. *Methods*, **19**, 373-385.

Yoshioka, K., Takahashi, H., Homma, T., Saito, M., Oh, K.-B., Nemoto, Y., and Matsuoka, H. (1996) A novel fluorescent derivative of glucose applicable to the assessment of glucose uptake activity of *Escherichia coli*. *Biochim. Biophys. Acta*, **1289**, 5-9.

A real-time method of imaging glucose uptake in single, living mammalian cells

Katsuya Yamada[1], Mikako Saito[2], Hideaki Matsuoka[2] & Nobuya Inagaki[3]

[1]Department of Physiology, Hirosaki University School of Medicine, Aomori 036-8562, and CREST of Japan Science and Technology Agency, Honcho 4-1-8, Kawaguchi, Saitama 332-0012, Japan. [2]Department of Biotechnology and Life Science, Tokyo University of Agriculture and Technology, 2-24-16 Nakamachi, Koganei, Tokyo 184-8588, and CREST, Japan. [3]Department of Physiology, Akita University School of Medicine, 1-1-1 Hondo, Akita 010-8543, and Department of Diabetes and Clinical Nutrition, Kyoto University Graduate School of Medicine, Kyoto, and CREST, Japan. Correspondence should be addressed to N.I. (inagaki@metab.kuhp.kyoto-u.ac.jp) about cell assays and to H.M. (mhide@cc.tuat.ac.jp) about 2NBDG synthesis.

Published online 29 March 2007; doi:10.1038/nprot.2007.76

This protocol details a method for monitoring glucose uptake into single, living mammalian cells using a fluorescent D-glucose derivative, 2-[*N*-(7-nitrobenz-2-oxa-1,3-diazol-4-yl)amino]-2-deoxy-D-glucose (2-NBDG), as a tracer. The specifically designed chamber and superfusion system for evaluating 2-NBDG uptake into cells in real time can be combined with other fluorescent methods such as Ca^{2+} imaging and the subsequent immunofluorescent classification of cells exhibiting divergent 2-NBDG uptake. The whole protocol, including immunocytochemistry, can be completed within 2 d (except for cell culture). The procedure for 2-NBDG synthesis is also presented.

INTRODUCTION

Glucose is the major carbon source used in the cells of most organisms, so measurement of glucose uptake is an important research issue. In mammalian cells in particular, measuring glucose uptake of a heterogeneous population and/or differing activity status is of great interest[1,2]. To quantify glucose uptake, a variety of radiolabeled tracers such as [^{3}H] glucose[2], [^{14}C] 2-deoxy-D-glucose (2-DG)[3], [^{18}F] fluoro-2-deoxy-D-glucose[4] and [^{14}C] or [^{3}H] 3-O-methyl-D-glucose[5,6] have been used effectively. However, the spatial and temporal resolution of these methods is not high, and they cannot be used to visualize glucose uptake in single, living cells.

This protocol details a method for real-time monitoring of glucose uptake in single mammalian cells using a fluorescent D-glucose derivative, 2-[*N*-(7-nitrobenz-2-oxa-1,3-diazol-4-yl)amino]-2-deoxy-D-glucose (2-NBDG), as a tracer. 2-NBDG was initially developed for the rapid non-culture count of viable microbial cells and was successfully applied to *Escherichia coli*[7] and many other food-borne bacteria[8]. It has since been demonstrated in living mammalian cells that the uptake of 2-NBDG takes place through glucose transporters (GLUTs) in a concentration-, time- and temperature-dependent manner[9]. A short-period application of 2-NBDG produced a remarkable increase in the fluorescence intensity in COS-1 cells over-expressing GLUT2, whereas the increase was barely detectable in mock-transfected cells[9]. In mouse insulin-secreting clonal MIN6 cells[10], uptake was inhibited by cytochalasin B, a specific blocker for GLUTs, and by D-glucose in a dose-dependent manner[9]. Kinetic analysis using fluorometry further revealed that the time course of the uptake into MIN6 cells was almost linear up to 2 min, and apparent K_m values calculated from the Eadie–Hofstee transformation using the initial velocity of uptake at 1 min were similar to those reported for D-glucose and the non-metabolizable glucose analog, 3-O-methyl-D-glucose, found in pancreatic islets and cultured β-cells[9].

In recent years, 2-NBDG has been shown to be useful for monitoring glucose uptake into a variety of mammalian cells. These include pig vascular smooth muscle cells[11], rabbit enterocytes[12], rat cardiomyocytes[13], rat and mouse astrocytes and neurons in culture and *in vivo*[14–18], human and murine tumor cell lines[19,20] and adipocyte cell lines[21]. Inhibition of 2-NBDG uptake by D-glucose has been confirmed using vascular smooth muscle cells[11] and tumor cell lines[20], and inhibition by cytochalasin B in rat astrocytes[15].

Direct visualization of glucose uptake without using isotopes makes the 2-NBDG method quite attractive[13,21,22]. In addition, 2-NBDG has recently been used to investigate cell type–specific uptake of glucose and intercellular communication, such as that in the CNS[14–16,18]. Simple superfusion of 2-NBDG over cells using a flow-through system allows simultaneous monitoring of differing glucose uptake into heterogeneous cells. However, care should be taken because fluorescence intensity is an arbitrary measure. Thus, quantification requires stability of the system as well as accurate procedures. Accordingly, we focus here on the construction of a flow-through system as well as a practical protocol for measurement of 2-NBDG uptake. Also presented are procedures for combining this method with Ca^{2+} imaging by fura-2 and subsequent immunocytochemical identification of cells[9].

The limitation in the use of 2-NBDG is related to its intracellular fate. We previously found that 2-NBDG is metabolized to a phosphorylated fluorescent derivative at the C-6 position (2-NBDG 6-phosphate) after entering into *E. coli* cells and then decomposes to a non-fluorescent derivative[23]. Thus, the fluorescence intensity should reflect a dynamic equilibrium of generation and decomposition of 2-NBDG and the fluorescent metabolite. The use of 2-NBDG in the study of intracellular glucose metabolism is thus limited, and experiments must be carefully performed.

The protocols for 2-NBDG synthesis are described as well as the detailed characteristics of 2-NBDG, for researchers who may want to use a large amount of purified 2-NBDG.

MATERIALS

REAGENTS

- DMEM containing 4,500 mg l^{-1} D-glucose (DMEM-HG) (Life Technologies, cat. no. 12800-082)
- MIN6 cells (see REAGENT SETUP)
- Ca^{2+}, Mg^{2+}-free (CMF) PBS (see REAGENT SETUP)
- Trypsin–EDTA (Life Technologies, cat. no. 25200-023)
- 2-NBDG (see **Box 1** and **Fig. 1**)
- Krebs Ringer bicarbonate buffer (KRB) (see REAGENT SETUP)

BOX 1 | SYNTHESIS OF 2-[*N*-(7-NITROBENZ-2-OXA-1,3-DIAZOL-4-YL)AMINO]-2-DEOXY-D-GLUCOSE (2-NBDG)

REAGENTS

- D-glucosamine (Sigma)
- $NaHCO_3$ (Kokusan Chemical)
- 4-Chloro-7-nitrobenzofurazan (NBD-Cl; Wako)
- Sephadex A-50 (Amersham Pharmacia)
- Sephadex LH-20 (Amersham Pharmacia)
- D_2O (100 atom %D; Aldrich)
- Acetonitrile (chromato-grade for thin-layer chromatography (TLC); Kokusan Chemical)
- Triethanolamine (TEA; Kokusan Chemical)
- TLC plate silica gel 60 F_{254} (Merck Japan Limited)

EQUIPMENT

- Rotary evaporator (N-1000; EYELA)
- Freeze-dryer (FD-1; EYELA)
- DEAE (2-(diethylamino)ethyl-) Sephadex A-50 column and Sephadex LH-20 column (see REAGENT SETUP below)

REAGENT SETUP

DEAE Sephadex A-50 column and Sephadex LH-20 column Equilibrate DEAE Sephadex A-50 and Sephadex LH-20 with dH_2O, and fill into respective glass columns according to the standard protocols recommended by the company. The resin volume is 30× 200 mm^2 (diameter times length) for DEAE Sephadex A-50 and 20 × 250 mm^2 (diameter times length) for Sephadex LH-20. Operate both columns according to the standard protocol of gel filtration.

PROCEDURE

1. Dissolve 0.5 g D-glucosamine in 10 ml 0.3 M $NaHCO_3$ solution in a 100-ml Erlenmeyer flask (solution A), and dissolve 0.5 g NBD-Cl in 20 ml methanol in a 50-ml beaker (solution B).
2. Mix solutions A (10 ml) and B (20 ml) in a 100-ml recovery flask (egg plant flask). Send N_2 gas into the flask to purge the inside air and finally seal the flask with a silicon rubber cork with a balloon filled with N_2 gas. Wrap the flask with aluminum foil to shield from light. Shake the flask in a water bath shaker at 30 °C for 18 h.
3. Remove precipitates in the reaction mixture by filtration through a nylon mesh (10 μm) (or glass wool) using an aspirator. Collect the filtrate in another recovery flask.
4. Evaporate the reaction mixture to remove the solvent. A slight amount of solvent remaining does not matter.
5. Add 10 ml dH_2O to the flask to dissolve the product (solution C).
6. Load solution C on the Sephadex A-50 column after filtration through a filter paper. Elute the column with dH_2O and collect yellow and orange fractions together. It is advisable to collect small fractions and then combine them after TLC (Step 7).
7. Frequently analyze the elute by TLC around the beginning and the end of the elution of yellow and orange components. This is done by performing these steps: (i) Spot 100-μl aliquots on the silica gel plate and develop with a solvent composed of $CH_3CN:H_2O$ = 17:3 (v/v). (ii) Detect fluorescent spots under a UV illuminator. (iii) Heat the plate to visualize sugar spots. (iv) Determine the retention factors (R_f) of fluorescent spots and sugar spots. A typical result is shown in **Figure 1a**. R_f of 2NBDG is 0.68.
Note: Maximize the 2NBDG yield but minimize the collection volume to be treated in the next step. Typically, the collection volume is approximately 200 ml (solution D).
8. Reduce the volume of solution D to about 5 ml by evaporation. Observe the solution volume carefully and stop evaporation before the volume becomes too small (this is solution E).
9. Load solution E on the Sephadex LH-20 column. Elute the column with dH_2O. Yellow, orange and brown fractions follow in that order. Collect the orange fractions.
10. Frequently analyze the eluate by HPLC around the beginning and the end of elution of the orange component. This is done by following these steps: (i) Inject 2–5-μl aliquots into the sample injection port and elute with solvent composed of $CH_3CN:H_2O$ = 17:3 (v/v). (ii) Adjust the elution speed to 0.5 ml min^{-1} and monitor the optical density of the eluate at 475 nm. A typical result is shown in **Figure 1b**. The peaks at 10.5 min (P_1) and 11.8 min (P_2) represent the β-D-anomer and α-D-anomer of 2-[*N*-(7-nitrobenz-2-oxa-1,3-diazol-4-yl)amino]-2-deoxy-D-glucose (2-NBDG), respectively. (iii) Estimate the purity using the formula (P_1 area + P_2 area)/(All peaks) × 100%.
Note: This is done to find the optimal condition to collect a maximum amount of 2-NBDG with highest purity. Successful gel filtration gives more than 98% purity.
11. Collect fractions containing 2-NBDG of more than 98% purity (solution F). Expected volume is 5 ml per fraction × 15–20 fractions.
Note: In case of low purity, repeat gel filtration using a fresh Sephadex LH-20 column.
12. Reduce the volume of solution F to approximately 10 ml by evaporation (solution G).
13. Freeze solution G in liquid N_2 to lyophilize the product. A yield of approximately 100 mg is expected.
Note: Dissolve the dry matter with dH_2O and store at 4 °C and use within 4 weeks. Keep the dry matter at −20 °C for longer storage.
14. Confirm the identity of the product by proton nuclear magnetic resonance analysis (^{1}H-NMR). Dissolve the dry matter of the product with deuterium oxide and immediately analyze it using ^{1}H-NMR under 500 MHz. A typical result is shown in **Figure 1c**. Assign peaks to respective protons of pyranose and NBD.

BOX 1 | CONTINUED

15. Analyze the mass spectrum by fast atom bombardment mass spectrometry (FAB-MS) (*m/z*) using triethanolamine as the matrix. Confirm the peak at 343 that corresponds to 2-NBDG-H^+.

16. Analyze the fluorescent spectrum according to the following steps: (i) Dissolve 2-NBDG with distilled water to adjust the concentration to 10 μg ml^{-1}. (ii) Measure emission spectrum from 495 to 650 nm under excitation at 475 nm. (iii) Measure the fluorescence intensity at 550 nm by scanning the excitation wavelength from 300 to 520 nm. (iv) Typical spectra depicted in **Figure 1d** will be obtained.

- D-Glucose (Wako)
- Cytochalasin B (Sigma, cat. no. C6762)

EQUIPMENT

- 35-mm culture dish with an oval glass bottom (14 × 5 mm^2, 0.08–0.12-mm-thick glass) (Matsunami Glass Ind., Osaka, Japan, cat. no. D110500) (**Fig. 2**) (see EQUIPMENT SETUP)
- Cover glass (cut into 10 × 11 mm^2 pieces) (Corning, cat. no. 1)
- Vacuum grease (HVAC-G; Shin-Etsu Silicone, Tokyo, Japan)
- Round-type, heating glass stage with a flat surface (0.5 mm thick, MPF-10HF) (Kitazato Supply, Fuji, Shizuoka, Japan) or equivalent
- Superfusate warmer (MT-1, dead volume = 0.13 ml; Narishige, Tokyo; or SF-28, Warner)
- Thermistor probe (IT-23, diameter = 0.23 mm; World Precision Instruments)
- Digital thermometer (TH-5; Physitemp Instruments, Clifton, NJ)
- Inverted microscope (Nikon DIAPHOT TMD300 or equivalent) equipped with long working distance (WD) objective lenses: Nikon CF Plan ×2 (NA 0.05, WD 5.8 mm), Plan ×4 DL (NA 0.13, WD 16.2 mm), Plan ×10 DL (NA 0.3, WD 9.2 mm) and Plan Fluor ×20 DLL Ph2 (NA 0.5, WD 2.1 mm) or Plan ELWD ×20 DL Ph2 (NA 0.4, WD 7.0–8.1 mm)
- Dichroic mirror (DM), excitation (Ex) and barrier (BA) filters used for 2-NBDG measurement are Nikon DM 505, Ex 480/40 and BA520–560, respectively
- Neutral density (ND) filters: Nikon ND2 (50%), ND4 (25%) and ND8 (12.5%) for fluorescent imaging; ND2 and ND16 (6.25%) for transmitted light imaging; variable intensity is obtained by using these filters in combination
- Peristaltic pump (MCP Standard pump equipped with 12 roller-pumphead MS/CA4-12; Ismatec SA, Glattbrugg, Switzerland)
- Vacuum pump (DAP-15; Alvac, Kanagawa, Japan)
- Vacuum pressure gauge
- Imaging system (Argus 50; Hamamatsu Photonics, Hamamatsu, Japan) or equivalent
- Silicon intensified target (SIT) camera (Hamamatsu Photonics) or equivalent

REAGENT SETUP

CMF-PBS NaCl, 137 g l^{-1}; KCl, 4.0 g l^{-1}; $NaH_2PO_42H_2O$, 0.36 g l^{-1}; KH_2PO_4, 0.18 g l^{-1}; $NaHCO_3$, 12 g l^{-1}; glucose, 11 g l^{-1}; pH 7.30–7.35.

KRB NaCl, 129 mM; KCl, 4.7 mM; KH_2PO_4, 1.2 mM; $CaCl_2$, 1.0 mM; $MgSO_4$, 1.2 mM; $NaHCO_3$, 5.0 mM; HEPES, 10 mM; pH 7.35–7.40.

Preparation of MIN6 cells (i) Prepare a total of 92 ml DMEM-HG containing 13% FBS (FBS-DMEM-HG) in two 50-ml tubes by adding 6 ml FBS to 40 ml DMEM-HG for each tube. (ii) Prepare two 10-cm culture dishes and add 10 ml FBS-DMEM-HG into each dish. (iii) Prepare 15 ml CMF-PBS. (iv) Prepare 1 ml trypsin–EDTA. (v) Warm (i–iv) at 37 °C for the following steps. (vi) Exchange medium in a 10-cm dish culturing MIN6 cells with 10 ml CMF-PBS. (vii) Suck CMF-PBS with a vacuum pump and add 5 ml CMF-PBS and 1 ml 0.25% trypsin–EDTA. (viii) After waiting for 1–2 min, peel off the cells gently by sucking and blowing the medium through a 10-ml pipette. (ix) Suck the cell suspension (approximately 6 ml) and transfer into 30 ml FBS-DMEM-HG. (x) Centrifuge at 1,500 r.p.m. for 3 min (in a Kubota 5200, Kubota Co., Tokyo, Japan). (xi) Suck the supernatant and add 10 ml FBS-DMEM-HG. (xii) Triturate five times with a 10-ml pipette (let cells go back and forth gently within the pipette using a Pipette aid). (xiii) Centrifuge at 1,500 r.p.m. for 1 min (in a Kubota 5200, Kubota Co., Tokyo, Japan). (xiv) Add 3 ml FBS-DMEM-HG. (xv) Triturate 40 times with a 5-ml pipette, and count cells within 30 s. (xvi) Dilute cell suspension at 20 × 10^4 ml^{-1}. (xvii) For passage, transfer 0.5 ml cell suspension into each of the 10-cm dishes containing 10 ml FBS-DMEM-HG (ii). (xviii) For the experiment, triturate 20 times again and transfer cell suspension (145 μl) onto the glass part of a glass-bottom culture dish. Moisten the glass part of the dish with 100 μl FBS-DMEM-HG beforehand and suck medium just before plating. (xix) Observe cells after waiting for 5 min and readjust the dilution ratio so that most cells are seen separately. If too many cells are observed, blow off cells with yellow tip and dilute again. (xx) Leave the cells in a CO_2 incubator (5% CO_2, 37 °C) for 30 min until the cells adhere to the glass. (xxi) Add 2 ml FBS-DMEM-HG to fill the whole culture dish. (xxii) Perform measurement of 2-NBDG uptake before many clusters of MIN6 cells are formed. To assess the health of MIN6 cells during the course of the passages, check [Ca^{2+}] responsiveness to glucose stimulation similarly to the procedure described in **Box 2** (**Figs. 2** and **3**).

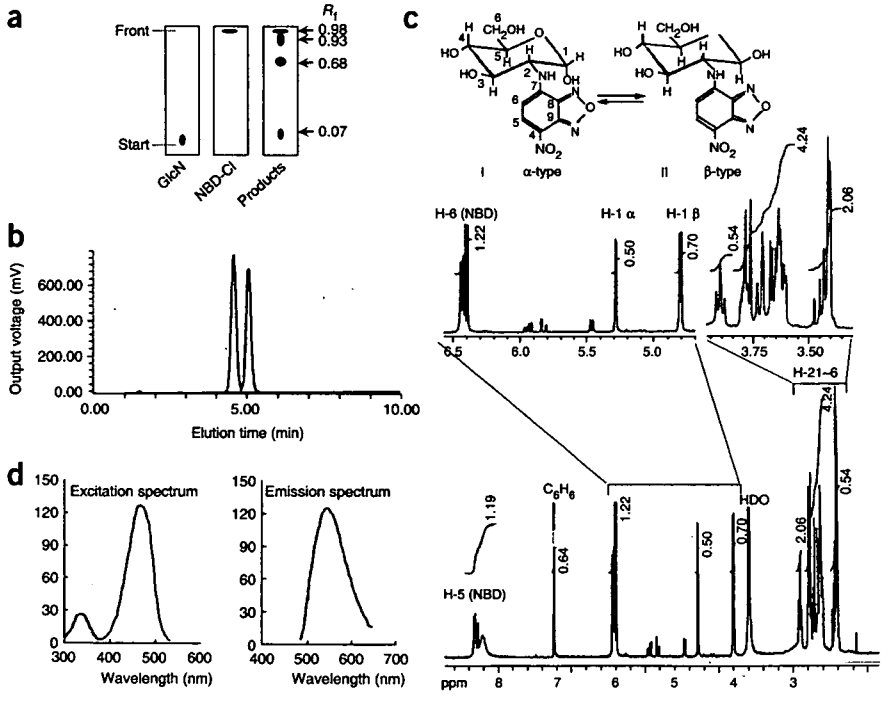

Figure 1 | Analytical data of 2-[*N*-(7-nitrobenz-2-oxa-1,3-diazol-4-yl)amino]-2-deoxy-D-glucose (2-NBDG). (**a**) TLC. Silica gel plate, solvent $CH_3CN:H_2O$ = 17:3, R_f (fluorescent spots: 2NBDG = 0.68, NBD-Cl = 0.98, GlcN = 0.07, unidentified by-products = 0.93). (**b**) HPLC spectrum. Column: TSKgel amide-80, eluent: $CH_3CN:H_2O$ = 17:3, flow rate: 1.0 ml min^{-1}, detection: $OD_{475\ nm}$. Two peaks: α-D-anomer and β-D-anomer. (**c**) ^1H-NMR spectrum. 500 MHz in D_2O, δ4.78 p.p.m. (d, $J_{1,2}$ = 10 c.p.s., axial–axial, β), δ5.27 p.p.m. (d, $J_{1,2}$ = 4 c.p.s., axial–equatorial, α), δ3.4–3.95 p.p.m. (m, H-2–H-6), δ6.4 p.p.m. (*m*, H-6 NBD), δ8.2–8.35 p.p.m. (*m*, H-5 NBD). (**d**) Fluorescence spectra. Emission spectrum: λ_{EM} = 495–650 nm, λ_{EX} = 475 nm; excitation spectrum: λ_{EM} = 550 nm, λ_{EX} = 300–520 nm.

Preparation of 2-NBDG solution Dissolve 2-NBDG in KRB (pH 7.35–7.40). The concentration of 2-NBDG and glucose should be determined according to the purpose of the experiment (see PROCEDURE). ▲ **CRITICAL** Do not freeze the 2-NBDG solution, as it will precipitate when thawing.

EQUIPMENT SETUP

Culture dish and superfusion chamber Mark random scratches beforehand on the outside of the oval glass bottom of the culture dish with a diamond knife for later immunocytochemical identification of the cells. Although a round glass-bottom culture dish can be used, the medium flow is smoother in an oval one. Prepare a plastic plate with a leaf-shaped hole, as the glass part of the dish is too shallow to obtain a stable medium flow (**Fig. 2**). This plate can be readily made using the culture dish by removing its glass bottom. Attach the plate tightly to the plastic part of the culture dish with vacuum grease just before experiment (see PROCEDURE). Thus, the depth of the glass part of the dish is doubled. A silicone rubber plate with an oval hole can be used instead of the plastic plate (**Fig. 2**). In this case, small projection portions made on the silicone plate (slashed part in **Fig. 2**) will help precise positioning of the cover glass.

Attach a square small cover glass (10 × 11 mm^2) to the plastic plate with a small amount of vacuum grease to cover the central part of the oval glass bottom (**Fig. 2**). The cover glass helps to smooth flow while decreasing the volume of superfusate, assuring rapid change of the solution, and also helps to prevent optical noise owing to fluctuation of the medium surface level. When only the central part of the bath is covered, drugs can be directly dropped onto the small gap upstream of the cover glass. In addition, local temperature at the region of interest below the cover glass can be easily checked during the experiment. ▲ **CRITICAL** Adjust the position, angle and height of the inlet and, especially, the outlet needle carefully (**Fig. 2**) to obtain smooth laminar flow.

Place a round, flat-surface heating glass stage on the microscope stage. A plastic holder plate (14 × 14 × 0.9 cm^3) with an opening (approximately 35 mm) in the central part should be fixed on the heating stage. The inner diameter of the opening must be determined by the outer diameter (sometimes tapered) of the dish used. Mount the culture dish into the plastic holder plate so that the glass bottom of the culture dish directly touches the heating glass stage (37 °C). Long-WD objective lenses (see EQUIPMENT) are required owing to the thickness of the heating glass stage.

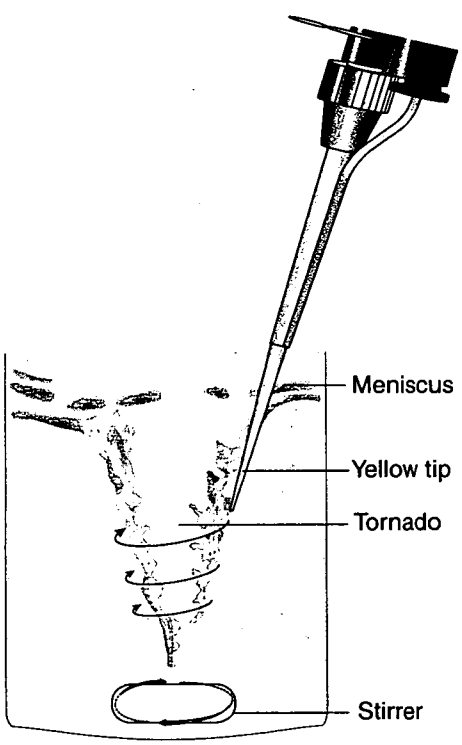

Figure 3 | Dissolving fura-2/AM in DMSO into Krebs Ringer bicarbonate buffer (KRB).

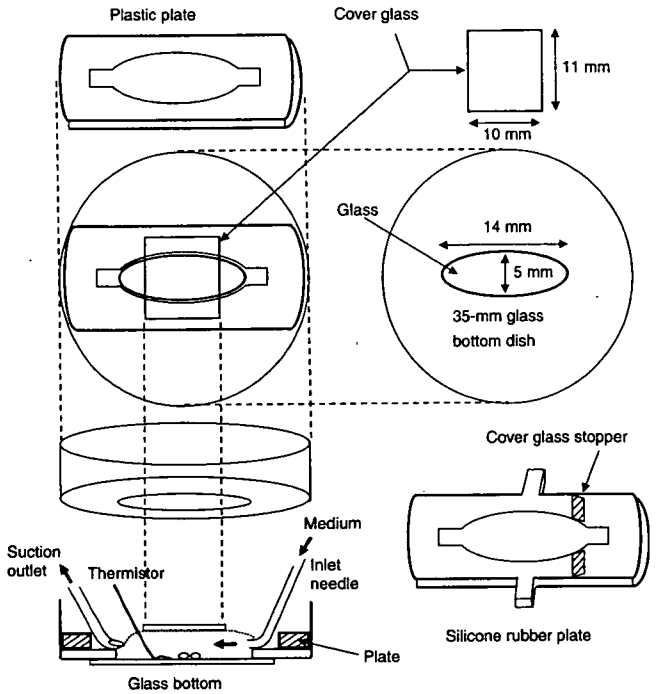

Figure 2 | A culture dish–based chamber for live-cell imaging. A plastic (or silicone rubber) plate is attached to the glass-bottom culture dish to make a bath for superfusion. The central part of the bath is covered by a cover glass to promote smooth flow and rapid exchange of superfusate.

Check the temperature of the superfusate at the region of interest by inserting a very thin thermistor probe between the cover glass and the glass bottom before (or sometimes during) the experiment. An extra dish with no cells should be prepared for just this purpose. Constant temperature at the area of interest (36.5–37.5 °C) indicates that the whole chamber system is working properly.

Use a low-pulsation peristaltic pump and a vacuum pump for the delivery and the removal of the superfusate, respectively. Substitution of the polyethylene tube with a stainless steel pipe of very thin internal diameter helps to decrease dead volume from the superfusate bottle to the dish. Adjust the vacuum pressure with a screw valve and/or three-way valves at 30–40 kPa so that cells are left on the dish. A simple delivery system using hydrostatic pressure can be used instead of a peristaltic pump. ▲ **CRITICAL** The shape of the end of the outlet needle for removing superfusate is critical to achieving a stable flow. The main consideration is that the hole at the end should be opened in the upward direction (**Fig. 2**). Bend a stainless steel needle (20G, 0.90 × 70 mm) smoothly so as not to interfere with smooth medium flow inside the needle. Then enlarge the hole at the end of the needle obliquely to the axis as large as is possible using sandpaper so that the needle has an elongated hole on the very tip. When the position and the angle of the needle are adequate, superfusate is sucked constantly from the hole together with air, making a constant sucking sound. We have designed a height-, angle- and rotation-adjustable small holder for the needle for this purpose (**Fig. 4**); this is available from Narishige Scientific Instruments, Tokyo, Japan (see **Table 1**).

PROCEDURE

Preparation for superfusion ⊛ TIMING 5 min

1| Take the culture dish out from the CO_2 incubator, and gently absorb the culture medium outside the glass bottom part of the dish. Then wipe the medium left on the plastic floor of the dish completely using a cotton swab, leaving medium only on the glass bottom part.

2| Attach the plastic plate with a leaf-shaped hole (**Fig. 2**) tightly to the culture dish with silicone vacuum grease.

BOX 2 | $[Ca^{2+}]_I$ MEASUREMENT COMBINED WITH MEASUREMENT OF 2-[*N*-(7-NITROBENZ-2-OXA-1,3-DIAZOL-4-YL)AMINO]-2-DEOXY-D-GLUCOSE (2-NBDG) UPTAKE IN PANCREATIC ISLET CELLS

REAGENTS

- Fura-2/AM (Dojindo, cat. no. 343-05401)
- DMSO (Dojindo)
- Ca^{2+}-free Krebs Ringer bicarbonate buffer (KRB) (see REAGENT SETUP below)
- $CaCl_2$ (0.1 M solution) (Wako)
- Glucose (Wako)
- Eagle's minimum essential medium containing kanamycin (60 μg ml^{-1}) (Nissui, cat. no. 1) and 5.6 mM glucose (MEM)
- EGTA (0.1 M solution) (Sigma, cat. no. E-4378)
- BSA (Fraction V, pH of 1% aqueous solution is 5.2) (Sigma, cat. no. A-4503)
- Tolbutamide (Sigma, cat. no. T0891)
- Guinea pig anti-swine insulin antibody (Dako, cat. no. N1542)
- Rabbit anti-porcine glucagon antibody (Dako, cat. no. L1813)
- Rhodamine-conjugated goat anti-rabbit IgG (Cappel)
- Rhodamine-conjugated goat anti-guinea pig IgG (Chemicon)
- Sodium phosphate buffer (PB)
- Paraformaldehyde (Nakalai)

EQUIPMENT

- Non-coated glass-bottom dishes
- Dichroic mirror and barrier filter (Nikon DM400) (BA510 LP)
- Excitation filter Hamamatsu MC340- and 380-nm excitation filters

REAGENT SETUP

Preparation of islet cells (i) Isolate islets of Langerhans from 8–12-week-old Harlan Sprague–Dawley rats by collagenase digestion under nembutal anesthesia[25]. (ii) Transfer the islets into ice-cold Ca^{2+}-free KRB containing 5.6 mM glucose. (iii) Centrifuge at 800 r.p.m. for 30–60 s (in a himac CR5B from Hitachi High Technologies, Tokyo, Japan) at room temperature (22–28 °C) and wash sediments with KRB containing 0.1 mM Ca^{2+}, 0.1% BSA and 5.6 mM glucose (repeat three times). A small addition of Ca^{2+} at this point will mitigate cellular damage by EGTA treatment in the next stage. (iv) Dissociate the islet into single cells by incubation for 15–17 min at room temperature in 200 μl Ca^{2+}-free KRB containing 1 mM EGTA, 0.1% BSA and 5.6 mM glucose. Make a 0.1 M EGTA stock solution for this purpose (adjust pH to 7.4 by 1 N HCl). (v) Triturate 8–12 times using a yellow tip. (vi) Transfer the dissociated islets into 10 ml of MEM supplemented with 10% FBS (MEM-FK). (vii) Centrifuge at 800 r.p.m. for 3 min (in a himac CR5B from Hitachi High Technologies, Tokyo, Japan) at room temperature, discard the supernatant by suction pipette and re-suspend the cells in 200 μl of MEM-FK. (viii) Plate a small amount of single cells (such as 30 μl) on a culture dish in the center of the oval glass bottom (**Fig. 2**). (ix) Leave the cells in a CO_2 incubator (5% CO_2, 37 °C) for 20 min until cells adhere to the glass bottom. (x) Add 0.5–1.0 ml of culture medium slowly. Cells can be maintained in the CO_2 incubator for up to 2 d. However, Ca^{2+} responsiveness to glucose stimulation is obtained from a maximal number of healthy β-cells during the several hours after plating.

Ca^{2+}-free KRB (mM) NaCl, 129; KCl, 4.7; KH_2PO_4, 1.2; $MgSO_4$, 1.2; $NaHCO_3$, 5.0; HEPES, 10; pH 7.35.

Preparation of fura-2/AM solution

1. Dissolve 10 μl 1 mM fura-2/AM in DMSO solution into 10 ml KRB containing 2.8 mM glucose and 1 mM Ca^{2+} (final concentration of fura-2/AM, 1 μM), as described.

Note: Use DMSO that has been kept dried, since moisture absorption interferes with dissolution of fura-2/AM (in DMSO) into aqueous solution. Detergents to promote dissolution such as Cremophor EL (C5135, Sigma) are not necessary. The volume of fura-2/AM-containing KRB should be determined according to the chamber volume and the total dead volume in the inlet tubing.

2. Stir vigorously 10 ml KRB solution in a small glass vial (such as 12.5 ml) using a very small stirrer magnet so that a stable, tornado-like vortex appears in the central part of the solution (**Fig. 3**). Use a high-performance magnetic stirrer.

Note: If a low-performance stirrer is used, the position of the vortex may move right or left unstably, and dissolution will be unsuccessful.

3. Push out the fura-2/DMSO solution continuously and as slowly as possible from a yellow tip. Hold the tip almost perpendicularly along, but slightly outside, the vortex wall. When dissolution is successful, fura-2/AM in DMSO disappears spirally into the KRB solution similar to a pale smoke or is almost unseen. Never suck the KRB into the tip by releasing pushing force.

Note: If water leaks into the tip, small oil droplets will be seen coming out from the tip into the KRB when fura-2/AM is pushed out, and the tip end will be polluted by white deposit. These droplets are due to undissolved fura-2, indicating unsuccessful dissolution. Discard the tip and try again from the beginning in such a case.

4. When subdivided into aliquots, keep fura-2/AM at below −20 °C in a tightly sealed box containing hygroscopic material to prevent moisture absorption during frequent use.

Preparation of glucose responsiveness experiment

1. Make KRB containing 1 mM Ca^{2+} as a superfusate during measurement. Make 100 ml of 0.1 M $CaCl_2$ stock solution to add Ca^{2+} to KRB. Prepare KRB containing 2.8 and 16.8 mM glucose.

2. Adjust pH of KRB stock solution to 7.3 with NaOH, because it will shift to 7.35–7.40 by the day of experiment.

Note: pH exceeding 7.4 may produce unsuccessful results.

BOX 2 | CONTINUED

3. Prepare tolbutamide in KRB by dissolving 1 M stock solution of tolbutamide (in DMSO) into KRB containing 2.8 mM glucose in a manner similar to that depicted in **Figure 3** (final concentration of tolbutamide, 200 μM).

PROCEDURE

Measurement of $[Ca^{2+}]_i$ in response to glucose stimulation: *fura-2/AM loading* ⊛ TIMING 30 min

1. Prepare 10 ml of KRB (depending upon the total dead volume in the inlet tubing) containing 2.8 mM glucose and 1 μM fura-2/AM for each culture dish.
2. Superfuse the islet cells with the fura-2/AM in KRB at a flow rate of 0.3 ml min^{-1} for 30 min at 37 °C.
3. Wash fura-2/AM solution with KRB containing 2.8 mM glucose at 37 °C. This protocol is both easy and time saving. Indeed, because only islet cells strongly adhered to the glass bottom are left on the dish after the loading, cells of interest can be searched for using the microscope immediately after fura-2/AM loading, which contributes to obtaining responses from cells still in a healthy condition.
4. As an alternative to the above method of loading fura-2/AM by superfusion, fura-2/AM can be loaded by exchanging culture medium with KRB containing 2.8 mM glucose and 1 μM fura-2/AM, and incubated for 30 min at 37 °C in a humidified atmosphere containing 5% CO_2 (in a CO_2 incubator).

Measurement of $[Ca^{2+}]_i$ in response to glucose stimulation: $[Ca^{2+}]_i$ measurement ⊛ TIMING 1 h

5. Superfuse KRB containing 2.8 mM glucose. Start searching the area of interest without waiting additional post-loading minutes for the hydrolysis of AM residue, as the searching process is usually time consuming.
6. Capture transmitted light images of cells of interest.
7. Start imaging the ratio F340/F380. Fura-2 fluorescence is detected every 5 or 10 s at 500–520-nm wavelength following excitation at 340-nm (F340) and 380-nm (F380) wavelengths. The ratio image is obtained using an Argus 50. (See Troubleshooting section below.)
8. Exchange superfusate to KRB containing 16.8 mM glucose for 5–10 min and then return to KRB containing 2.8 mM glucose.
9. After the ratio recovers to baseline for about 10 min or so, check responsiveness of β-cells to tolbutamide by superfusing KRB containing 200 μM tolbutamide for a brief period within 30 s.

Measurement of 2-NBDG uptake ⊛ TIMING 30–60 min

10. After finishing Ca^{2+} imaging, start measurement of 2-NBDG uptake in a manner similar to that described for MIN6 cells. To discriminate β-cells from other cell types, KRB containing 200 μM 2-NBDG and 2.8 mM glucose is loaded for 1 min. Quenching of fura-2 fluorescence is not required since the 2-NBDG fluorescence is strong enough in comparison with fura-2 fluorescence, and the 2-NBDG uptake is evaluated by the relative increase in the fluorescence.

ANTICIPATED RESULTS

A raw example of measurement of $[Ca^{2+}]_i$ and subsequent 2-NBDG uptake in pancreatic islet cells is shown in **Figure 6**. After loading fura-2/AM by superfusion, a region of interest is selected and a transmitted light image is captured (**Fig. 6a**). Cells to be monitored are then selected on the fluorescent image (**Fig. 6b**). Information on the $[Ca^{2+}]_i$ response to glucose stimulation (**Fig. 6c**) and the subsequent uptake of 2-NBDG by a brief superfusion (**Fig. 6d,e**) were used to evaluate the divergent uptake of heterogeneous islet cells in combination with later immunocytochemistry (**Fig. 6f**). Since islet cells consist of a heterogeneous population of cells, including glucose-responsive insulin-secreting β-cells and glucose-unresponsive glucagon-secreting α-cells as well as somatostatin-secreting δ-cells, later immunocytochemical identification of cell type is essential (see **Box 3**).

TROUBLESHOOTING

Problem: Extraordinary large ratio in $[Ca^{2+}]_i$ imaging.
Possible reason: Unhealthy cells may show a large ratio. Especially important, islet cells do not remain healthy for many hours in KRB containing 2.8 mM glucose. In addition, care should be taken to prevent high-temperature degradation of the coating materials of the emission filter, which can be continuously exposed to heat radiation from the xenon lamp during the experiment despite the heat-insulating lens.
Solution: Carry out experiments using freshly prepared cells. To retard degradation of the coating materials of the filter, empty the home filter position and use two heat-insulating lenses in the pathway from the lamp. The condition of the filters should be checked by making a calibration curve for $[Ca^{2+}]_i$.

⚠ **CRITICAL STEP** A toothpick and a small bent spatula can be used to spread the grease and press the plate, respectively. If you use too much grease, it comes out from the gap between the dish and the plate and interferes with medium flow. If you use too little, the superfusate leaking into the gap will interfere with smooth exchange of the superfusate during drug application, which is especially problematic when high concentrations of 2-NBDG are applied.

3| Cover the central part of the oval glass bottom with a square cover glass with a small amount of vacuum grease (**Fig. 2**).

4| Mount the dish on the plastic holder on the inverted microscope stage and start superfusion immediately with KRB containing 5.6 mM glucose. Paint a small mark on the rim of the dish so that it coincides with the mark on the holder. This makes it possible to reproduce the angle of the dish when immunocytochemistry is conducted later.

BOX 3 | IMMUNOCYTOCHEMICAL IDENTIFICATION OF ISLET CELLS AFTER MEASUREMENT OF 2-[*N*-(7-NITROBENZ-2-OXA-1,3-DIAZOL-4-YL)AMINO]-2-DEOXY-D-GLUCOSE (2-NBDG) UPTAKE

REAGENTS

- Guinea pig anti-swine insulin antibody (Dako, cat. no. N1542)
- Rabbit anti-pig glucagon antibody (Dako, cat. no. L1813)
- Rhodamine-conjugated goat anti-guinea pig IgG (Chemicon)
- Rhodamine-conjugated goat anti-rabbit IgG (Cappel)
- Sodium phosphate buffer (PB)
- Paraformaldehyde (Nakalai)

EQUIPMENT

- Dichroic mirrors and filters: Nikon DM575 (EX 510–560, BA 590 LP)

Immunocytochemistry ⏱ TIMING 5 h–4.5 d

1. At the end of the measurement of 2-NBDG uptake, capture transmitted light images of the analyzed cells at ×20, ×10, ×4 and ×2 for immunocytochemical identification of their location. Low-magnification lenses are especially convenient for finding the analyzed region in reference to the scratches previously made under the glass bottom of the culture dish.
2. Fix cells in cold 0.1 M PB containing 2% paraformaldehyde overnight at 4 °C. Alternatively, pour the cold fixative on the cells and leave cells for up to 1 h at room temperature.
3. Wash three times (rotate the dish gently and wait for 5 min between each washing) with 0.01 M PBS. Cells may be treated with 1% BSA.
4. React cells with primary antibodies, such as guinea pig anti-pig insulin antibody (1:100) or rabbit anti-pig glucagon antibody (prediluted), at room temperature for 1 h or at 4 °C overnight.

Note: Can be left up to 3 d at 4 °C.

5. React with rhodamine-conjugated secondary antibody (1:100–1:500) at room temperature for 1 h.
6. Wash three times with PBS.
7. Mount the dish on the plastic holder on the microscope stage so that the mark on the rim of the dish coincides with the mark on the holder.
8. Show the previous low-magnification image of the cells on the PC monitor and affix tiny triangles made of opaque tape on both ends of individual major scratches observed on the monitor screen. Then find the same scratch pattern by microscope and adjust the field of view so that the identical pattern is seen on the monitor using the opaque triangles as guides. Finer adjustment can be made by comparing the current image with the previous image. Repeat the process in higher-magnification views.
9. Examine rhodamine fluorescence.

ANTICIPATED RESULTS

See **Figure 6f.**

Measurement of 2-NBDG uptake ⏱ TIMING 30–60 min

5| Select area of interest and capture a transmitted light image.

6| Demarcate cells. Select an area for evaluating changes in background fluorescence.

7| Adjust the gain of the detection system and capture fluorescent images. A transmitted light image with no ND filter is useful for identifying locations of cells on the monitor screen by the intrinsic fluorescence of the cells. Strong ND filters are used when the fluorescence of cells is saturated after loading 2-NBDG.

8| Superfuse MIN6 cells with glucose-free KRB for 15 min.

9| Change superfusate to D-glucose-free KRB containing 50–600 μM 2-NBDG for 15–120 s, and then wash.

⚠ **CRITICAL STEP** The concentration of 2-NBDG and the loading period are to be determined according to the purpose of the experiment, the type of GLUTs of interest and the signal-to-noise ratio of the detection system. For the signal-to-noise ratio and the superfusion technique used in the present system, the shortest practical loading period is 15 s, and the smallest concentration is 50 μM. When 600 μM 2-NBDG is used, a loading period longer than 120 s should be avoided because of the nonlinear increase in the 2-NBDG fluorescence over time[9]. With a system requiring a long loading period (e.g., tens of minutes),

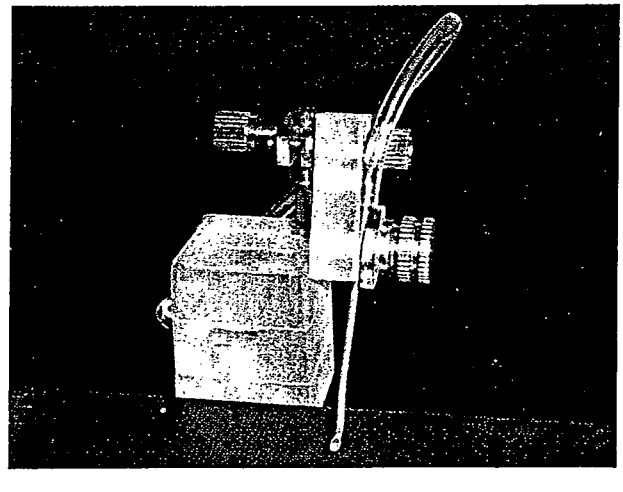

Figure 4 | A custom-made holder for the outlet needle (Narishige). Height, rotation angle and lean angle of the needle are freely adjustable without using a screwdriver.

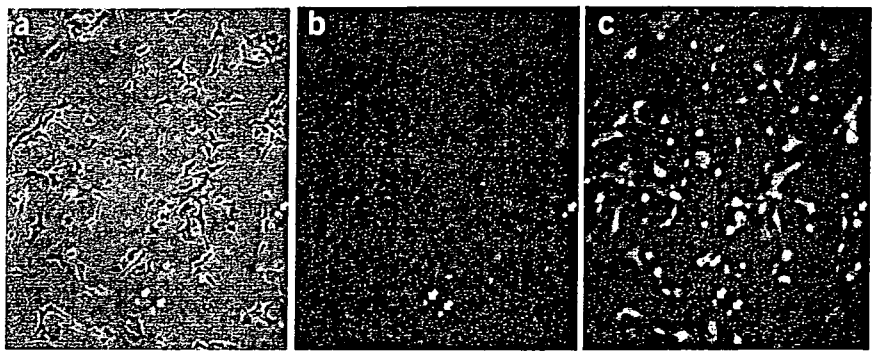

Figure 5 | Measurement of 2-[*N*-(7-nitrobenz-2-oxa-1,3-diazol-4-yl)amino]-2-deoxy-D-glucose (2-NBDG) uptake into MIN6 cells. (**a**) Transmitted light image (×20). Arrows indicate debris of dead cells. Raw fluorescent images measured at 540-nm wavelength with no neutral density (ND) filter (**b**) before and (**c**) after loading Krebs Ringer bicarbonate buffer (KRB) containing 600 μM 2-NBDG for 15 s. Note that no increase in the fluorescence intensity is seen for the debris (arrows). The field of view in the fluorescent images (**b**) and (**c**) was narrowed by the diaphragm in the fluorescent light path.

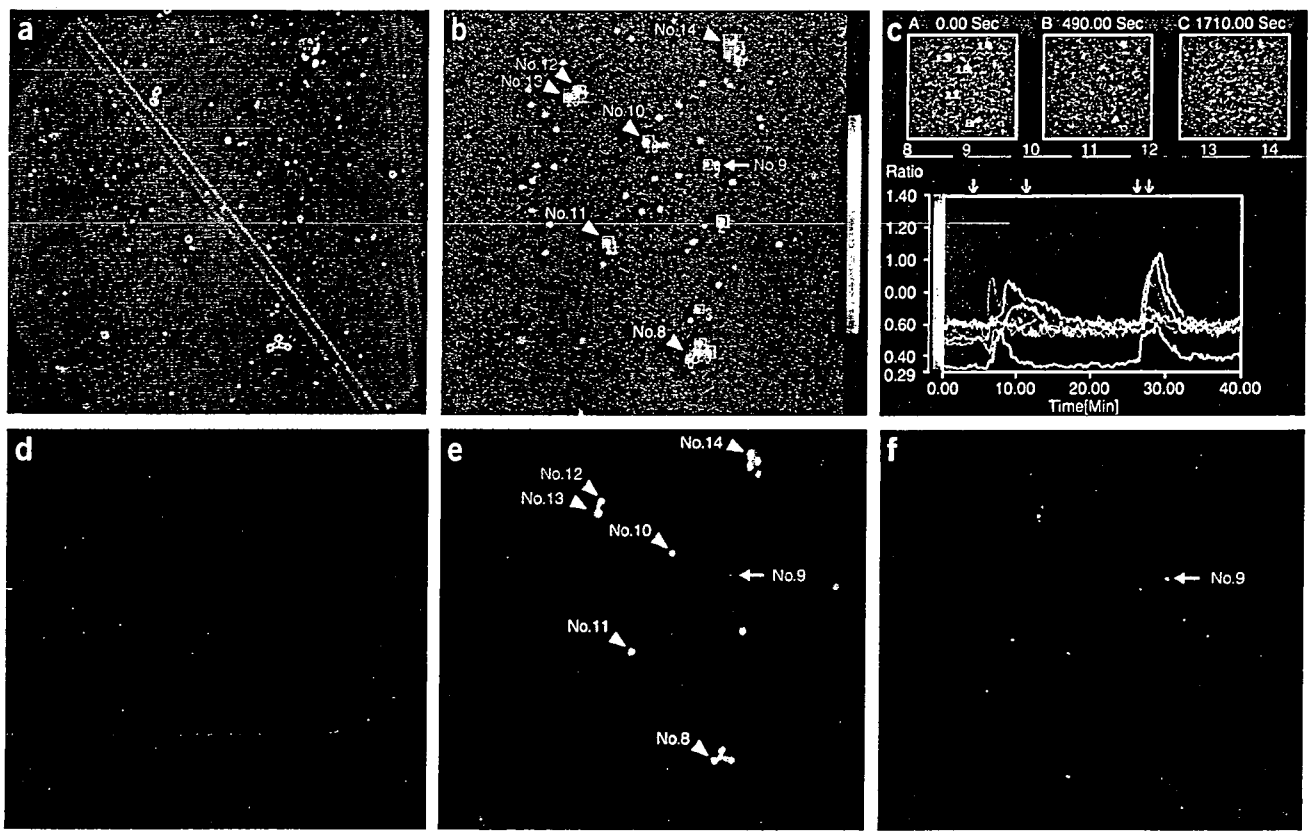

Figure 6 | Measurement of $[Ca^{2+}]_i$ in response to glucose stimulation and subsequent 2-[*N*-(7-nitrobenz-2-oxa-1,3-diazol-4-yl)amino]-2-deoxy-D-glucose (2-NBDG) uptake in living pancreatic islet cells followed by immunocytochemical identification. (**a**) Transmitted light image (×20). Scratches made under the glass bottom of the dish are visible. (**b**) Raw fluorescent image examined at 500–520-nm wavelength for 380-nm excitation after loading of 1 μM fura-2/AM by superfusion. Areas demarcated by squares were tentatively selected for monitoring $[Ca^{2+}]_i$ responses before starting the measurement. Of these, the responses of cells indicated by colored numbers are exemplified (see below). (**c**) A window of the Argus 50 for $[Ca^{2+}]_i$ analysis. Seven areas can be analyzed on one page of the Argus 50 (seven colors are assigned automatically). Areas showing increases (no. 8 and nos. 10–14) and no increase (no. 9) in $[Ca^{2+}]_i$ are expressed as the change in fura-2 fluorescence ratio (340 or 380 nm) (lower panel). Small downward arrows above the lower panel indicate periods of superfusing Krebs Ringer bicarbonate buffer (KRB) containing 16.8 mM glucose (between the two left arrows) and 200 μM tolbutamide (between the right arrows). The response times to tolbutamide coincided for cells responding to high glucose, whereas the response times to glucose varied, indicating accuracy of the superfusion and differences in intracellular metabolism after glucose uptake among cells. Upper insets are provided by the software for checking locations of cells and changes in the fluorescence at different time points. Fluorescent images measured at 540-nm wavelength (**d**) before and (**e**) after loading 200 μM 2-NBDG for 1 min. Cells incorporating 2-NBDG are β-cells[9], and uptake of 2-NBDG into cell no. 9 was undetectable during 1 min loading. (**f**) Immunocytochemistry of glucagon. Rhodamine-conjugated secondary antibody was used. Cell no. 9 (arrow) was clearly immunopositive for glucagon. Rhodamine fluorescence was examined with a 590-nm longpass filter (excitation wavelength 510–560 nm). Note that the location of the cells incorporating abundant 2-NBDG can be identified by their vague fluorescence. In (**a**–**e**), cells were superfused continuously with KRB containing 2.8 mM glucose at 37 °C, and the KRB was supplemented as indicated. In these original pictures, no subtraction or shading correction was done. Contrast was adjusted for clarity only in panels (**d**) and (**e**). Note that some cells were lost and some not seen in the original transmitted light image entered from upstream during superfusion. Some of these data were first published in ref. 9.

some investigators use a very low concentration of 2-NBDG (10 μM)[13]. For a long loading period, time-dependent extinction should also be considered. In MIN6 cells, the intensity of 2-NBDG fluorescence (200 μM loaded for 60 s) was linearly decreased to 87.7, 70.9 and 56.6% 15, 30 and 60 min after uptake, respectively, under dark condition (K. Yamada and N. Inagaki, unpublished data). Care should be taken that the actual loading period of 2-NBDG from the beginning of superfusion to complete washing is constant for all of the cells compared. Differences in the local temperature within the area of interest should be within 1 °C (e.g., 36.5–37.5 °C) to minimize temperature-dependent variance of the uptake[9].

? TROUBLESHOOTING

10| When 2-NBDG uptake is evaluated in the presence of glucose, skip Step 8 and change the superfusate to KRB containing 2-NBDG and glucose. The glucose concentration added to the KRB should be determined according to the purpose of experiment. To test inhibition of 2-NBDG uptake by D-glucose, superfuse cells with KRB containing 11.2 mM D-glucose and compare the 2-NBDG uptake with that in the absence of D-glucose. The uptake of 2-NBDG (600 μM loaded for 2 min) in the presence of 11.2 mM glucose was significantly inhibited by 52.5 ± 6.3% compared with uptake in the absence of glucose[9].

11| After washing for 5 min, capture fluorescent images.

12| Calculate the relative fluorescence intensity of each cell before and after loading 2-NBDG by subtracting the corresponding background fluorescence from the fluorescence intensity of the cells.

13| Calculate the net increase in the fluorescence intensity for each cell by subtracting the relative fluorescence intensity before from that after loading 2-NBDG.

14| To test whether the 2-NBDG uptake occurs through GLUTs, superfuse cells with KRB containing 10 μM cytochalasin B 5 min before the 2-NBDG loading. In MIN6 cells, the increase in fluorescence by loading 200 μM 2-NBDG for 15 s was almost completely inhibited in the presence of cytochalasin B[9].

? TROUBLESHOOTING

Troubleshooting advice can be found in **Table 1.**

TABLE 1 | Troubleshooting table.

Step	Problem	Possible reasons	Solution
9	Variable results in 2-[*N*-(7-nitrobenz-2-oxa-1,3-diazol-4-yl)amino]-2-deoxy-D-glucose (2-NBDG) fluorescence in quantitative measurements or high background fluorescence due to 2-NBDG	Unstable superfusion in the chamber	Check for smooth superfusion by dropping a small amount of dye such as pontamine sky blue (Brilliant Blue 6B, CI-24420, Tokyo Chemical Industry, Tokyo, Japan) using an extra dish without cells. Adjust the position of the outlet needle so that it slightly protrudes into the glass bottom part. Adjust the inlet angle and direction finely so that a smooth, laminar flow is obtained. A constant sound of sucking of the superfusate from the outlet needle indicates a stable flow. Measure the temperature of each region of interest with a thin thermistor probe to confirm that the temperature difference is within 1 °C. An area meeting this criterion can be marked on the cover glass. Measurement of the local temperature also helps in finding irregular flow
		Pollution by 2-NBDG fluorescence from the forceps used for placing and removing the plastic plate on the glass-bottom culture dish, or other materials such as the thermistor probe	Every time a dish is exchanged, the plate and forceps used should be rinsed thoroughly. Make several additional plates to save time. Each time vacuum grease is taken from the tube, use a new disposable toothpick so that the grease itself is not polluted by 2-NBDG fluorescence. Similar care should be taken for other parts
		Variance of uptake specific to the particular cell types of interest	See ANTICIPATED RESULTS

ANTICIPATED RESULTS

An example of the raw measurements of 2-NBDG uptake in MIN6 cells is shown in **Figure 5.** The fluorescence of MIN6 cells, which was only slightly discernible before loading, was remarkably increased by a brief (15 s) superfusion of 600 μM 2-NBDG in the absence of glucose. In the transmitted light image, cells with an abnormal round shape are easily distinguished from normal cells exhibiting irregular shape[24]. Abnormal cells and areas where multiple cells are overlapping are to be excluded from the

analysis. MIN6 cells exhibit a relatively homogeneous uptake of 2-NBDG. However, when other cell types are used, care should be taken to determine whether the variable uptake of 2-NBDG is due to intrinsic differences in the glucose uptake of individual cells (**Box 2**, **Box 3** and **Fig. 6**).

ACKNOWLEDGMENTS We are grateful to our collaborators, Drs. Masanori Nakata and Naoki Horimoto. We also thank Drs. K. Yoshizaki and S. Sato for technical help, and Dr. J. Miyazaki (Osaka University) for providing us with MIN6 cells.

COMPETING INTERESTS STATEMENT The authors declare no competing financial interests.

Published online at http://www.natureprotocols.com
Reprints and permissions information is available online at http://npg.nature.com/reprintsandpermissions

1. Sokoloff, L. Sites and mechanisms of function-related changes in energy metabolism in the nervous system. *Dev. Neurosci.* **15**, 194–206 (1993).
2. Heimberg, H., De Vos, A., Pipeleers, D., Thorens, B. & Schuit, F. Differences in glucose transporter gene expression between rat pancreatic a- and b-cells are correlated to differences in glucose transport but not in glucose utilization. *J. Biol. Chem.* **270**, 8971–8975 (1995).
3. Sokoloff, L. *et al.* The [^{14}C]deoxyglucose method for the measurement of local cerebral glucose utilization: theory, procedure, and normal values in the conscious and anesthetized albino rat. *J. Neurochem.* **28**, 897–916 (1977).
4. Turkheimer, F. *et al.* The use of spectral analysis to determine regional cerebral glucose utilization with positron emission tomography and [^{18}F]fluorodeoxyglucose: theory, implementation, and optimization procedures. *J. Cereb. Blood Flow Metab.* **14**, 406–422 (1994).
5. Dienel, G.A., Cruz, N.F., Adachi, K., Sokoloff, L. & Holden, J.E. Determination of local brain glucose level with [^{14}C]methylglucose: effects of glucose supply and demand. *Am. J. Physiol.* **273**, E839–E849 (1997).
6. Axelrod, J.D. & Pilch, P.F. Unique cytochalasin B binding characteristics of the hepatic glucose carrier. *Biochemistry* **22**, 2222–2227 (1983).
7. Yoshioka, K. *et al.* A novel fluorescent derivative of glucose applicable to the assessment of glucose uptake activity of *Escherichia coli*. *Biochim. Biophys. Acta* **1289**, 5–9 (1996).
8. Matsuoka, H. *et al.* Viable cell detection by the combined use of fluorescent glucose and fluorescent glycine. *Biosci. Biotechnol. Biochem.* **67**, 2459–2462 (2003).
9. Yamada, K. *et al.* Measurement of glucose uptake and intracellular calcium concentration in single, living pancreatic β-cells. *J. Biol. Chem.* **275**, 22278–22283 (2000).
10. Miyazaki, J. *et al.* Establishment of a pancreatic beta cell line that retains glucose-inducible insulin secretion: special reference to expression of glucose transporter isoforms. *Endocrinology* **127**, 126–132 (1990).
11. Lloyd, P.G., Hardin, C.D. & Sturek, M. Examining glucose transport in single vascular smooth muscle cells with a fluorescent glucose analogue. *Physiol. Res.* **48**, 401–410 (1999).
12. Roman, Y., Alfonso, A., Carmen Louzao, M., Vieytes, M.R. & Botana, L.M. Confocal microscopy study of the different patterns of 2-NBDG uptake in rabbit enterocytes in the apical and basal zone. *Eur. J. Physiol.* **443**, 234–239 (2001).
13. Ball, S.W., Bailey, J.R., Stewart, J.M., Vogels, C.M. & Westcott, S.A. A fluorescent compound for glucose uptake measurements in isolated rat cardiomyocytes. *Can. J. Physiol. Pharmacol.* **80**, 205–209 (2002).
14. Loaiza, A., Porras, O.H. & Barros, L.F. Glutamate triggers rapid glucose transport stimulation in astrocytes as evidenced by real-time confocal microscopy. *J. Neurosci.* **23**, 7337–7342 (2003).
15. Bernardinelli, Y., Magistretti, P.J. & Chatton, J.-Y. Astrocytes generate Na^+-mediated metabolic waves. *Proc. Natl. Acad. Sci. USA* **101**, 14937–14942 (2004).
16. Porras, O.H., Loaiza, A. & Barros, F. Glutamate mediates acute glucose transport inhibition in hippocampal neurons. *J. Neurosci.* **24**, 9669–9673 (2004).
17. Itoh, Y., Abe, T., Takaoka, R. & Tanahashi, N. Fluorometric determination of glucose utilization in neurons *in vitro* and *in vivo*. *J. Cereb. Blood Metab.* **24**, 993–1003 (2004).
18. Blomstrand, F. & Giaume, C. Kinetics of endothelin-induced inhibition and glucose permeability of astrocyte gap junctions. *J. Neurosci. Res.* **83**, 996–1003 (2006).
19. O'Neil, R.G., Wu, L. & Mullani, N. Uptake of a fluorescent deoxyglucose analogue (2-NBDG) in tumor cells. *Mol. Imaging Biol.* **7**, 388–392 (2005).
20. Cheng, Z. *et al.* Near-infrared fluorescent deoxyglucose analogue for tumor optical imaging in cell culture and living mice. *Bioconjug. Chem.* **17**, 662–669 (2006).
21. Nakata, M. *et al.* Effects of statins on the adipocyte maturation and expression of glucose transporter 4 (SLC2A4): implications in glycaemic control. *Diabetologia* **49**, 1881–1892 (2006).
22. Zou, C., Wang, Y. & Shen, Z. 2-NBDG as a fluorescent indicator for direct glucose uptake measurement. *J. Biochem. Biophys. Methods* **64**, 207–215 (2005).
23. Yoshioka, K. *et al.* Intracellular fate of 2-NBDG, a fluorescent probe for glucose uptake activity, in *Escherichia coli* cells. *Biosci. Biotech. Biochem.* **60**, 1899–1901 (1996).
24. Minami, K. *et al.* Insulin secretion and differential gene expression in glucose-responsive and -unresponsive MIN6 sublines. *Am. J. Physiol. Endocrinol. Metab.* **279**, E773–E781 (2000).
25. Yada, T., Itoh, K. & Nakata, M. Glucagon-like peptide-1-(7-36)amide and a rise in cyclic adenosine 3,5-monophosphate increase cytosolic free Ca^{2+} in rat pancreatic beta-cells by enhancing Ca^{2+} channel activity. *Endocrinology* **133**, 1685–1692 (1993).

Journal of Applied Microbiology ISSN 1364-5072

ORIGINAL ARTICLE

Evaluation of a new medium for the enumeration of total coliforms and *Escherichia coli* in Japanese surface waters

H. Kodaka[1,2], S. Mizuochi[1], M. Saito[2] and H. Matsuoka[2]

1 Research Institute of Advanced Technology, Nissui Pharmaceutical Co. Ltd, Hokunanmoro, Yuki, Ibaraki, Japan
2 Department of Biotechnology and Life Science, Tokyo University of Agriculture and Technology, Nakamachi, Koganei, Tokyo, Japan

Keywords
coliforms, EC-Blue-10, *E. coli*, enumeration, MPN, water.

Correspondence
Hidemasa Kodaka, Research Institute of Advanced Technology, Nissui Pharmaceutical Co. Ltd, 1075-2, Hokunanmoro, Yuki, Ibaraki 307-0036, Japan.
E-mail: h-kodaka@yki.nissui-pharm.jp

2007/0564: received 10 April 2007, revised and accepted 20 September 2007

doi:10.1111/j.1365-2672.2007.03627.x

Abstract

Aim: A new medium, EC-Blue-10, containing chromogenic and fluorogenic substrates, KNO_3 and sodium pyruvate has been developed for the rapid simultaneous detection and enumeration of total coliforms and *Escherichia coli* in water.

Methods and Results: Two evaluations of EC-Blue-10 were carried out. Firstly, EC-Blue-10 was compared with Colilert-MPN for 96 water samples using MPN for total coliforms and *E. coli*. Secondly, the detection of coliforms and *E. coli* were compared using 2400 tubes of EC-Blue-10 and Colilert-MPN. The regression coefficients between EC-Blue-10 and Colilert-MPN for total coliforms and *E. coli* were 0·91 and 0·89, respectively. For the detection results, the Cohen's kappa values between the two media were 0·79 for coliforms and 0·72 for *E. coli*.

Conclusions: EC-Blue-10 is almost same as Colilert-MPN for the detection of coliforms and *E. coli* in surface waters. Further evaluation for EC-Blue-10 is needed to verify in different geographical areas.

Significance and Impact of the Study: EC-Blue-10 is useful method for the rapid and simultaneous detection of total coliforms and *E. coli* in water sample.

Introduction

Total coliforms and *Escherichia coli* are important indicators of the sanitary quality of drinking water. The standard test for the coliform group is either the multiple-tube fermentation technique (Grasso *et al.* 2000) or the membrane-filter technique (Bernasconi *et al.* 2006). Since traditional multiple-tube fermentation and membrane-filter methods require a minimum of 24 h incubation followed by a confirmation procedure lasting 24–48 h, there is a requirement for rapid test methods for the emergency testing of drinking water supplies. During recent decades new chromogenic or fluorogenic, defined substrate methods based on β-galactosidase for total coliforms or β-glucuronidase for *E. coli* and ready-made culture media have been introduced (Edberg and Edberg 1988). Many chromogenic media based on β-galactosidase for total coliforms use *o*-nitrophenol-β-D-galactopyranoside (ONPG) or chlorophenol red-β-D-galactopyranoside (CPRG) as a substrate. The results of studies comparing media containing ONPG or CPRG and 4-methylumbelliferyl-β-D-glucuronide (MUG) with standard methods (Edberg *et al.* 1988; Buckalew *et al.* 2006) provide critical information confirming the accuracy of the defined substrate technology (DST) method, its comparability to a standard method, and its applicability for use. ONPG could be replaced successfully by 5-bromo-4-chloro-3-indoxyl-β-D-galactopyranoside (X-Gal) (Manafi and Kneifel 1989). However, there are few studies testing commercially available liquid media that use X-Gal and MUG for the simultaneous determination of total coliforms and *E. coli* in water (Manafi and Kneifel 1989; Geissler *et al.* 2000; Hörman and Hänninen 2006). We have developed a new medium using X-Gal and MUG for rapidly and simultaneously detecting total coliforms and *E. coli* in water. EC-Blue-10 is a new medium in a special